Error estimates for a viscosity-splitting scheme in time applied to non-Newtonian fluid flows

Mofdi El-Amrani[a], Anouar Obbadi[a], Mohammed Seaid[b,*], Driss Yakoubi[c]

[a]*Laboratory of Mathematics and Applications, FSTT, Abdelmalek Essaadi University, Tangier, Morocco*
[b]*Department of Engineering, University of Durham, South Road, DH1 3LE, United Kingdom*
[c]*Léonard de Vinci Pôle Universitaire, Research Center, 92 916 Paris La Défense, France*

Abstract

A time fractional-step method is presented for numerical solutions of the incompressible non-Newtonian fluids for which the viscosity is non-linear depending on the shear-rate magnitude according to a generic model. The method belongs to a class of viscosity-splitting procedures and it consists of separating the convection term and incompressibility constraint into two time steps. Unlike the conventional projection methods, the viscosity is not dropped in the last step allowing to enforce the full original boundary conditions on the end-of-step velocity which eliminates any concerns about the numerical boundary layers. We carry out a rigorous error analysis and provide a full first-order error estimate for both the velocity and pressure solutions in the relevant norms. Numerical results are presented for two test examples of non-Newtonian fluid flows to demonstrate the theoretical analysis and confirm the reliability of this viscosity-splitting scheme.

Keywords: Fractional-step methods; Non-Newtonian fluids; Navier-Stokes equations; Viscosity-splitting schemes; Error estimates.

1. Introduction

During the past decade, there has been an increasing awareness about the incapability of the Newtonian assumption to explain the observed behavior of many fluids encountered in industrial activities such as slurry transportation and polymeric melts [1]. Since then a growing interest has been devoted to this large category of substances which turns out to be far more widespread in real-life than the Newtonian ones, examples include biological fluids like blood and saliva, chocolates, wet beach sand, printing ink, cosmetic products like lotions and shampoos, mineral suspensions, among others. In general a fluid behavior is highly impacted by the relation between the shear stress and the shear rate, and while it is linear for the Newtonian fluids with the so-called dynamic viscosity as the proportionality constant, this

*Corresponding author
Email addresses: `mofdi.elamrani@gmail.com` (Mofdi El-Amrani), `anouar.obbadi@etu.uae.ac.ma` (Anouar Obbadi), `m.seaid@durham.ac.uk` (Mohammed Seaid), `driss.yakoubi@devinci.fr` (Driss Yakoubi)

relation is much more complex in the non-Newtonian fluids and it can vary from one to another yielding a diverse range of characteristics to each fluid flow. In addition, the generalized Newtonian fluids convene the fluids preserving the tensorial structure of the Newtonian class but their apparent viscosity is no longer constant but a function of the shear-rate magnitude. Thus, the shear stress-shear rate relationship is determined based only on the viscosity response to the applied shear rate. The generalized Newtonian fluids whose viscosity decreases when experiencing an increase in the shear rate are known by shear-thinning (or pseudoplastic) fluids and are the most common in realistic applications whereas, the so-called shear-thickening (or dilatant) fluids exhibits an opposite behavior as their apparent viscosity increases with the shear rate. In practice, dilatant fluids are a less widespread subclass than the pseudoplastics and can be encountered for example in thick suspensions.

Recently, several mathematical models, mostly based on rheological data, have been proposed in the literature to formally describe features and dynamics of the non-Newtonian fluids. Some of the commonly used for time-independent fluids include the power law (or Ostwald de Waele) model, the Cross model [2], the Carreau model, the Ellis model and others that can be found for example in [3, 4]. Regardless of the adopted model, it is straightforwardly injected into the motion equations of the fluid, precisely into the diffusion term, resulting in a class of non-linear incompressible Navier-Stokes equations that are even more challenging than their Newtonian counterparts which are already hard to tackle, especially in three space dimensions, even with the computational resources of nowadays. The difficulty in solving these problems lies mainly on the saddle-point structure of the governing equations and the non-linearities of the convective and of the viscous terms in the case of non-Newtonian fluids. One of the most popular approaches proposed in the literature to address these difficulties is the projection, or splitting, or fractional-step methods initiated by the leading works of Chorin [5] and Temam [6] in the late 60s. The basic idea consists of decoupling the diffusion term and the incompressibility constraint through two (or more) time-marching steps. In the first step, the pressure and the incompressibility constraint are canceled out to compute an intermediate velocity which is projected later in the second step, after dropping the viscous term, on a divergence-free space by solving a Poisson-type equation for the pressure. However, the resulting non-physical boundary conditions on the pressure deteriorate the accuracy and the convergence orders of the method even with high-order time integration schemes. Therefore, authors in [7] proposed a pressure-correction strategy that introduces an old pressure term in the first step of the splitting and then corrects accordingly in the second step, which indeed improved the accuracy but issues related to the inconsistent pressure boundary conditions still persisted and defected the pressure approximation especially when the problem under study is equipped with open boundaries. To overcome these drawbacks, a rotational version of the pressure-correction method was suggested in [8] which efficiently removed the inconsistency and enhanced the $\mathbf{H}^1$-norm accuracy of the velocity and the L^2-norm accuracy of the pressure (see [9]) even with open boundary conditions (see [10]). Other techniques based on improved pressure boundary conditions were presented in [11, 12] to resolve these problems. Alternatively, a viscosity-splitting approach was proposed in [13] which consists of separating the convective term from the incompressibility constraint in the first step and then injects a viscous term in the second step. The introduced diffusion term, albeit compromises the simple Poisson structure of the incompressibility step in the classical projection methods, it also allows to enforce the full original boundary conditions on the end-of-step velocity and consequently, it avoids any artificial boundary conditions. It should be noted that authors in [13] also supplemented their method with a pressure-correction modification.

It should also be stressed that investigating the performance of fractional-step methods solving the non-Newtonian fluids is of great interest as complex fluids are largely involved in the industry emphasizing a necessity to accurately monitor their flow behavior in various geometries and configurations. However, this task is not straightforward since strengths of this method can be neutralized by the non-homogeneous or the shear-rate dependent viscosity, see for example [14] and further discussions are therein. On the other hand, the literature relevant to this research field is rather scarce and, when it comes to the error analysis, is almost nonexistent. It should be stressed that by properly modifying the pressure Poisson equation, authors in [14] extended the pressure-correction method to the case of non-homogeneous viscosity and succeeded to numerically retrieve the same performance as the rotational version through what they called the shear-rate projection techniques. This method has also been generalized in [15] to account for open-boundary conditions and shear-rate dependent viscosity. Another efficient splitting method was developed in [16] based on the technique studied earlier in [17] that replaces the incompressibility constraint by a Poisson-type equation for the pressure equipped with consistent boundary conditions and results in decoupling the computation of the velocity and pressure solutions. Other research works that directly applied the non-incremental or the incremental conventional projection methods combined with different spatial discretizations for various generalized Newtonian models can be found for example in [18, 19, 20, 21, 22] among other. It should be noted that, in all the previous literature, no convergence analysis and error estimates are reported for the non-Newtonian case except evidence based on computational results.

In the present study, we first extend the viscosity-splitting technique presented in [13] to generalized Newtonian fluids whose viscosity follows the Carreau model. Next, we develop a rigorous analysis of convergence for this method and provide error estimates for both the velocity and pressure solutions. To the best of our knowledge, error estimates for the viscosity-splitting method solving non-Newtonian fluid flows are reported for the first time. To evaluate the accuracy of the viscosity-splitting scheme, we present numerical results for a three-dimensional problem with known exact solution and also for the two-dimensional benchmark problem of forward-facing step flow. The obtained results for different flow regimes are in good agreement with our theoretical expectations and illustrate good numerical behaviors in terms of stability and accuracy. The remainder of this paper is structured as follows: the viscosity-splitting for non-Newtonian fluid flows is presented in Section 2. This section includes the governing mathematical equations, notations along with functional spaces and assumptions used in the current work. The error estimates for the considered viscosity-splitting scheme are established in Section 3. In this section we prove a first-order error estimates for the velocity solution in both L^2- and H^1-norms as well as a first-order convergence for the pressure solution in the L^2-norm. Numerical results obtained for two test examples of non-Newtonian fluid flows are illustrated in Section 4. Conclusions are summarized in Section 5.

2. Viscosity-splitting scheme for non-Newtonian fluid flows

Let Ω be a bounded domain $\Omega \subset \mathbb{R}^d$ ($d = 2, 3$) with Lipschitz continuous boundary $\partial\Omega$, and $[0, T]$ be the time interval with $T > 0$ is the final time. In what follows, we use the whole scale of Sobolev spaces $W^{m,q}(\Omega)$, with $m \geq 0$ and $1 \leq q \leq +\infty$ equipped with the norm $\|\cdot\|_{W^{m,q}(\Omega)}$ and semi-norm $|\cdot|_{W^{m,q}(\Omega)}$, which reduces to the usual notation $H^m(\Omega)$ when $q = 2$ with the corresponding norm $\|\cdot\|_m$. We also require the space $H_0^1(\Omega)$ of functions in $H^1(\Omega)$ vanishing on $\partial\Omega$. It should be noted that thanks to the Poincare's inequality, the norm $\|\cdot\|_1$ and semi-norm $|\cdot|_1$ are equivalent in $H_0^1(\Omega)$. Furthermore, we define the vector spaces

$$\boldsymbol{H} = \left\{\mathbf{v} \in \boldsymbol{L}^2(\Omega), \quad \nabla\cdot\mathbf{v} = 0, \quad \mathbf{v}\cdot\mathbf{n}|_{\partial\Omega} = 0\right\},$$

where $\mathbf{n}$ is the unit outward normal vector to the boundary $\partial\Omega$, and

$$\boldsymbol{V} = \left\{\mathbf{v} \in \mathbf{H}_0^1(\Omega);\ \nabla\cdot\mathbf{v} = 0\right\}.$$

To account for the homogeneous pure Dirichlet boundary conditions, we also define the zero-mean space

$$L_0^2(\Omega) = \left\{q \in L^2(\Omega);\ \int_\Omega q d\boldsymbol{x} = 0\right\}.$$

In the present study, we consider an unsteady flow of a generalized Newtonian fluid with a non-homogeneous viscosity ν depending on time t, space $\boldsymbol{x}$, velocity $\boldsymbol{u}(t, \boldsymbol{x})$, shear rate of the fluid $\mathbf{D}\boldsymbol{u}$, the fluid pressure $p(t, \boldsymbol{x})$ and/or other external quantities and subject to a constitutive equation of the form

$$\sigma(\boldsymbol{u}) = -p\mathbf{I} + 2\nu\mathbf{D}\boldsymbol{u},$$

where $\mathbf{I}$ is the unit matrix and the shear rate is defined as

$$\mathbf{D}\boldsymbol{u} = \frac{1}{2}\left(\nabla\boldsymbol{u} + \nabla\boldsymbol{u}^\top\right).$$

Assuming incompressible flows, the the Navier-Stokes equations read

$$\begin{aligned} \frac{\partial\boldsymbol{u}}{\partial t} + (\boldsymbol{u}\cdot\nabla)\boldsymbol{u} - \nabla\cdot(2\nu\mathbf{D}\boldsymbol{u}) + \nabla p &= \mathbf{f}, \qquad (t, \boldsymbol{x}) \in (0, T] \times \Omega, \\ \nabla\cdot\boldsymbol{u} &= 0, \qquad (t, \boldsymbol{x}) \in (0, T] \times \Omega, \end{aligned} \tag{1}$$

where $\mathbf{f} \in L^2\left(0, T; \mathbf{L}^2(\Omega)\right)$ is an external force such as gravity. The equations (1) are equipped with an homogeneous Dirichlet-type boundary condition on $\partial\Omega$ as

$$\boldsymbol{u}(t, \boldsymbol{x}) = \mathbf{0}, \qquad (t, \boldsymbol{x}) \in (0, T] \times \partial\Omega, \tag{2}$$

and an initial condition as

$$\boldsymbol{u}(0, \mathbf{x}) = \boldsymbol{u}_0(\mathbf{x}), \qquad \boldsymbol{x} \in \Omega, \tag{3}$$

where $\boldsymbol{u}_0(\mathbf{x}) \in \mathbf{L}^2(\Omega)$ is a given initial function. It should be stressed that the existence and regularity of the solution for the case of Newtonian fluids has been studied in [23, 24, 25] among others. In the case of non-Newtonian fluids, existence of a solution of the problem (1)-(3) has been proved under some assumptions on the viscosity ν, see for example [25, 26, 27]. In the current work, we consider the generic law

$$\nu(\mathbf{D}\boldsymbol{u}) = \nu_\infty + (\nu_0 - \nu_\infty)\left(\lambda_0 + \lambda^2 \|\mathbf{D}\boldsymbol{u}\|^2\right)^{\frac{m-1}{2}}, \tag{4}$$

where m, λ_0, ν_∞ and ν_0 are nonnegative constants to be selected for each type of fluid, and $\|\cdot\|$ denotes the Euclidean norm in $\mathbb{R}^{d\times d}$. Notice that in all the theoretical results presented in the current work, we assume that $m \leq 1$ which covers a wide family of shear-thinning fluids whose viscosity is decreasing with the shear rate.

Note that the relation (4) covers a wide range of rheological models used in various industrial applications and it also verifies the assumptions required in [25, 26, 27] for the existence of a solution for (1)-(3). Here, based on the analysis reported in [27], the existence of a weak solution of (1)-(3) is ensured provided $m > 0$ for $d = 2$ and $m > 1/5$ for $d = 3$.

For the time integration of equations (1)-(3), the time interval $[0, T]$ is divided into K sub-intervals $[t_k, t_{k+1}]$ with length $\Delta t = t_{k+1} - t_k$, $0 = t_0 < t_1 < \cdots < t_K = T$, and we use the notation $\boldsymbol{w}^k = \boldsymbol{w}(t_k, \boldsymbol{x})$ as the value of a generic function w at time t_k. We aslo define the discrete norms in a Banach space X as

$$\|u\|_{l^2(0,T;X)} = \left(\Delta t \sum_{k=0}^{K} \left\|u^k\right\|_X^2\right)^{\frac{1}{2}} \qquad \text{and} \qquad \|u\|_{l^\infty(0,T;X)} = \max_{0\leq k\leq K} \left\|u^k\right\|_X.$$

Applied to equations (1)-(3), the viscosity-splitting method is carried out using the following two steps:

Step 1: Given $\boldsymbol{u}^k$ at time t_k, compute the intermediate velocity $\widetilde{\boldsymbol{u}}^{k+1}$ as

$$\begin{aligned} \frac{\widetilde{\boldsymbol{u}}^{k+1} - \boldsymbol{u}^k}{\Delta t} + \boldsymbol{u}^k \cdot \nabla\widetilde{\boldsymbol{u}}^{k+1} - \nabla \cdot \left(2\nu\left(\mathbf{D}\boldsymbol{u}^k\right)\mathbf{D}\widetilde{\boldsymbol{u}}^{k+1}\right) &= \mathbf{f}^{k+1}, \qquad \boldsymbol{x} \in \Omega, \\ \widetilde{\boldsymbol{u}}^{k+1} &= 0, \qquad \boldsymbol{x} \in \partial\Omega. \end{aligned} \tag{5}$$

Step 2: Given $\widetilde{\boldsymbol{u}}^{k+1}$ from **Step 1**, compute the solution $\left(\boldsymbol{u}^{k+1}, p^{k+1}\right)$ of the Stokes problem as

$$\begin{aligned} \frac{\boldsymbol{u}^{k+1} - \widetilde{\boldsymbol{u}}^{k+1}}{\Delta t} - \nabla \cdot \left(2\nu\left(\mathbf{D}\boldsymbol{u}^k\right)\left(\mathbf{D}\boldsymbol{u}^{k+1} - \mathbf{D}\widetilde{\boldsymbol{u}}^{k+1}\right)\right) + \nabla p^{k+1} &= 0, \qquad \boldsymbol{x} \in \Omega, \\ \nabla \cdot \boldsymbol{u}^{k+1} &= 0, \qquad \boldsymbol{x} \in \Omega, \\ \boldsymbol{u}^{k+1} &= 0, \qquad \boldsymbol{x} \in \partial\Omega. \end{aligned} \tag{6}$$

Some remarks are in order:

i. In the first step, the convection and diffusion terms are treated in a semi-implicit fashion which eliminates the non-linearities that would have required a fixed point-like processing.

ii. The viscosity term included in the second step yields a Stokes-like problem which, albeit being more complex to solve than the Poisson problem required in the standard projection methods [5, 6, 28], it cancels any inconsistent boundary conditions on the pressure and it removes errors in the tangential boundary conditions thanks to the third equation in (6).

iii. The second step can also be interpreted as a projection of the intermediate velocity $\widetilde{\boldsymbol{u}}^{k+1}$ onto an $\mathbf{H}^1$-space, instead of an $\mathbf{L}^2$-space (known as Helmoltz decomposition [29]) in the standard projection methods, by rewriting the first equation in (6) as

$$\widetilde{\boldsymbol{u}}^{k+1} = \boldsymbol{u}^{k+1} + \Delta t \mathcal{P}^{-1} \nabla p^{k+1},$$

where $\mathcal{P}^{-1} \in \mathcal{L}\left(\boldsymbol{H}^{-1}(\Omega); \boldsymbol{H}_0^1(\Omega)\right)$ is the inverse of the operator $\mathcal{P}$ whose expression is given by

$$\mathcal{P} : \mathbf{v} \longrightarrow \mathbf{v} - \Delta t \nabla \cdot \left(2\nu(\boldsymbol{D}\boldsymbol{u}^k)\boldsymbol{D}\boldsymbol{v}\right),$$

and it is related to an homogeneous Dirichlet problem, *i.e.* for a given $\boldsymbol{\omega}$ in $\boldsymbol{H}^{-1}(\Omega)$, $\mathbf{v} = \mathcal{P}^{-1}\boldsymbol{\omega}$ is equivalent to $\mathbf{v}$ being the solution of the problem

$$\begin{aligned} \mathcal{P}\mathbf{v} &= \boldsymbol{\omega}, && \text{in } \Omega, \\ \mathbf{v} &= 0, && \text{on } \partial\Omega. \end{aligned}$$

Similarly, the above viscosity-splitting method can be formulated in a weak form as:

Step 1: Assume that the solution $\boldsymbol{u}^k \in \mathbf{H}_0^1(\Omega)$ is known, then the weak form of (5) is: find $\widetilde{\boldsymbol{u}}^{k+1} \in \mathbf{H}_0^1(\Omega)$ such that

$$\left(\frac{\widetilde{\boldsymbol{u}}^{k+1} - \boldsymbol{u}^k}{\Delta t}, \mathbf{v}\right) + \left(\boldsymbol{u}^k \cdot \nabla \widetilde{\boldsymbol{u}}^{k+1}, \mathbf{v}\right) + \left(2\nu\left(\mathbf{D}\boldsymbol{u}^k\right)\, \mathbf{D}\widetilde{\boldsymbol{u}}^{k+1}, \mathbf{D}\mathbf{v}\right) = \left(\mathbf{f}^{k+1}, \mathbf{v}\right), \qquad \text{for all} \quad \mathbf{v} \in \mathbf{H}_0^1(\Omega). \tag{7}$$

Step 2: Given $\widetilde{\boldsymbol{u}}^{k+1} \in \mathbf{H}_0^1(\Omega)$, the weak form of (6) is: find the solution $\left(\boldsymbol{u}^{k+1}, p^{k+1}\right)$ of the Stokes problem as

$$\begin{aligned} \left(\frac{\boldsymbol{u}^{k+1} - \widetilde{\boldsymbol{u}}^{k+1}}{\Delta t}, \mathbf{v}\right) + \left(2\nu\left(\mathbf{D}\boldsymbol{u}^k\right)\left(\mathbf{D}\boldsymbol{u}^{k+1} - \mathbf{D}\widetilde{\boldsymbol{u}}^{k+1}\right), \mathbf{D}\mathbf{v}\right) - \left(p^{k+1}, \nabla \cdot \mathbf{v}\right) &= 0, && \text{for all} \quad \mathbf{v} \in \mathbf{H}_0^1(\Omega), \\ \left(\nabla \cdot \boldsymbol{u}^{k+1}, q\right) &= 0, && \text{for all} \quad q \in L_0^2(\Omega). \end{aligned} \tag{8}$$

It should be stressed that the above time-splitting scheme can be modified to account for a pressure-correction procedure by treating the pressure explicitly in the first step and then making a correction in the second step. Although this modification does improve the accuracy of the approximate solution, it has no advantage on the expected order of the method, see [30] for further discussions. Therefore, we chose not to include it here for the sake of simplicity and clearness since the focus of the present work is mainly on the error estimates of the viscosity-splitting scheme for solving the non Newtonian fluid flows.

2.1. Well-posedness for the weak problem

In this section, the well-posedness of the system (7)-(8) is proved in the case of $m \leq 1$. Let a_0 be the bilinear form on $\mathbf{H}_0^1(\Omega) \times \mathbf{H}_0^1(\Omega)$, $\widetilde{l}$ the linear form on $\mathbf{H}_0^1(\Omega)$ and c the trilinear form on $\left(\mathbf{H}_0^1(\Omega)\right)^3$ defined by

$$a_0(\boldsymbol{w}, \mathbf{v}) = \frac{1}{\Delta t}(\boldsymbol{w}, \mathbf{v}) + \left(2\nu\left(\mathbf{D}\boldsymbol{u}^k\right)\mathbf{D}\boldsymbol{w}, \mathbf{D}\mathbf{v}\right), \qquad c\left(\boldsymbol{u}^k, \boldsymbol{w}, \mathbf{v}\right) = \left(\boldsymbol{u}^k \cdot \nabla \boldsymbol{w}, \mathbf{v}\right), \qquad \widetilde{l}(\mathbf{v}) = (\mathbf{f}^{k+1}, \mathbf{v}) + \frac{1}{\Delta t}\left(\boldsymbol{u}^k, \mathbf{v}\right).$$

Hence, the problem (7) can be rewritten as: find $\widetilde{\boldsymbol{u}}^{k+1} \in \mathbf{H}_0^1(\Omega)$ such that

$$\widetilde{a}\left(\widetilde{\boldsymbol{u}}^{k+1}, \mathbf{v}\right) = \widetilde{l}(\mathbf{v}), \qquad \text{for all} \quad \mathbf{v} \in \mathbf{H}_0^1(\Omega), \tag{9}$$

where

$$\widetilde{a}\left(\widetilde{\boldsymbol{u}}^{k+1}, \mathbf{v}\right) = a_0(\widetilde{\boldsymbol{u}}^{k+1}, \mathbf{v}) + c\left(\boldsymbol{u}^k, \widetilde{\boldsymbol{u}}^{k+1}, \mathbf{v}\right).$$

Since $\boldsymbol{u}^k$ is supposed to be in $\mathbf{H}_0^1(\Omega)$, the continuity of $\widetilde{l}$ is guaranteed by the Cauchy-Schwarz inequality, and the continuity of c is also established by virtue of the Holder's inequality in addition to the continuous embedding of $\mathbf{H}^1(\Omega)$ in $\mathbf{L}^4(\Omega)$. Moreover, the trilinear form c satisfies the following continuity properties on $\left(\mathbf{H}_0^1(\Omega)\right)^3$ (see for instance [31]) that can be useful later

$$c(\boldsymbol{u}, \mathbf{v}, \boldsymbol{w}) \leq \begin{cases} C\,|\boldsymbol{u}|_1\,|\mathbf{v}|_1\,|\boldsymbol{w}|_1\,, \\ C\,\|\boldsymbol{u}\|_0\,\|\mathbf{v}\|_2\,|\boldsymbol{w}|_1\,, \\ C\,|\boldsymbol{u}|_1\,\|\mathbf{v}\|_2\,\|\boldsymbol{w}\|_0\,, \\ C\,\|\boldsymbol{u}\|_0\,|\mathbf{v}|_1\,\|\boldsymbol{w}\|_2\,, \\ C\,\|\boldsymbol{u}\|_2\,|\mathbf{v}|_1\,\|\boldsymbol{w}\|_0\,, \\ C\,|\boldsymbol{u}|_1\,|\mathbf{v}|_1\,\|\boldsymbol{w}\|_0^{1/2}\,|\boldsymbol{w}|_1^{1/2}, \end{cases} \tag{10}$$

where C is a constant that depends on the domain Ω. In what follows, C denotes a generic positive constant independent of the time step Δt but it may depend on the problem data and it may have a different expression at each occurrence. In addition to the continuity properties, the trilinear form c is also a skew-symmetric in its last two arguments if the first argument lies in the space $\boldsymbol{H}$, *i.e.*

$$c(\boldsymbol{u}, \mathbf{v}, \mathbf{v}) = 0, \qquad \forall\ \mathbf{v} \in \mathbf{H}^1(\Omega), \qquad \forall\ \boldsymbol{u} \in \boldsymbol{H},$$

which is true in our case since $\boldsymbol{u}^k$ is also divergence-free. Hence,

$$c(\boldsymbol{u}^k, \mathbf{v}, \mathbf{v}) = 0, \qquad \forall\ \mathbf{v} \in \mathbf{H}_0^1(\Omega). \tag{11}$$

To establish the continuity of a_0, let g be a positive function defined by

$$g(s) = \nu_\infty + (\nu_0 - \nu_\infty)\left(\lambda_0 + \lambda^2 s^2\right)^{\frac{m-1}{2}}.$$

Obviously, when $\nu_0 \geq \nu_\infty$, the function $g(s) \geq \nu_\infty$ for all $s \in \mathbb{R}$ and, under the condition $m \leq 1$, the function g is upper bounded by a positive constant independent of Δt as

$$g(s) \leq \nu_\infty + (\nu_0 - \nu_\infty)\,\lambda_0^{\frac{m-1}{2}}, \qquad \forall\ s \in \mathbb{R}.$$

Hence, there exists a constant $C > 0$ such that

$$|a_0\,(\boldsymbol{w}, \mathbf{v})| = \left|\left(2g\left(\left\|\mathbf{D}\boldsymbol{u}^k\right\|^2\right)\mathbf{D}\boldsymbol{w}, \mathbf{D}\mathbf{v}\right)\right| \leq C\,|\boldsymbol{w}\,|_1|\,\mathbf{v}|_1\,,$$

and the continuity of the form $\widetilde{a}$ is proved. In addition, the coercivity of a_0 results from the lower bound of g and the Korn's inequality which straightforwardly lead to the coercivity of the form $\widetilde{a}$ since $c\left(\boldsymbol{u}^k, \mathbf{v}, \mathbf{v}\right) = 0$. Consequently, the problem (7) is well-posed by virtue of Lax Milgram's theorem.

The weak formulation (8) can be reformulated as: find $\left(\boldsymbol{u}^{k+1}, p^{k+1}\right) \in \mathbf{H}_0^1(\Omega) \times L_0^2(\Omega)$ such that

$$\begin{aligned} a_0\left(\boldsymbol{u}^{k+1}, \mathbf{v}\right) + b(p^{k+1}, \mathbf{v}) &= l(\mathbf{v}), \qquad \forall \mathbf{v} \in \mathbf{H}_0^1(\Omega), \\ b\left(q, \boldsymbol{u}^{k+1}\right) &= 0, \qquad \forall q \in L_0^2(\Omega), \end{aligned} \tag{12}$$

where

$$l(\mathbf{v}) = a_0\left(\widetilde{\boldsymbol{u}}^{k+1}, \mathbf{v}\right), \qquad b\,(q, \boldsymbol{w}) = -\,(q, \nabla \cdot \boldsymbol{w})\,, \qquad \forall q \in L_0^2(\Omega), \quad \forall \boldsymbol{w} \in \mathbf{H}_0^1(\Omega).$$

Since the continuity and the coercivity of the bilinear form a_0 are already established, and since the inf-sup condition on the bilinear form b is well known to be satisfied (see for example [32, 33]), we conclude the well-posedness of (12) and equivalently the problem (8) is well-posed.

2.2. *Stability of the time integration*

The aim here is to show the continuous dependency of the solution of (7)-(8) with respect to the initial data of the problem (*i.e.*, $\boldsymbol{u}_0$ and $\mathbf{f}$) which is expressed by the following lemma:

Lemma 2.1. *The intermediate and the end-of-step velocities satisfy*

$$\begin{aligned} \|\boldsymbol{u}_0\|_0^2 + \frac{\Delta t\, C_p^2}{2C_r \nu_\infty} \sum_{k=0}^{K-1} \|\boldsymbol{f}^{k+1}\|_0^2 \;\geq\; & \|\boldsymbol{u}^K\|_0^2 + \sum_{k=0}^{K-1} \|\boldsymbol{u}^{k+1} - \widetilde{\boldsymbol{u}}^{k+1}\|_0^2 + \sum_{k=0}^{K-1} \|\widetilde{\boldsymbol{u}}^{k+1} - \boldsymbol{u}^k\|_0^2 + \\ & 2C_r \nu_\infty \Delta t \sum_{k=0}^{K-1} \|\nabla(\boldsymbol{u}^{k+1} - \widetilde{\boldsymbol{u}}^{k+1})\|_0^2 + 2C_r \nu_\infty \Delta t \sum_{k=0}^{K-1} \|\nabla \boldsymbol{u}^{k+1}\|_0^2, \end{aligned}$$

where C_r is the constant of the Korn's inequality and C_p is the constant of Poincaré's inequality.

Proof. Taking $\mathbf{v} = 2\Delta t \widetilde{\boldsymbol{u}}^{k+1}$ in (7) and considering (11), one gets

$$\|\widetilde{\boldsymbol{u}}^{k+1}\|_0^2 - \left\|\boldsymbol{u}^k\right\|_0^2 + \left\|\widetilde{\mathbf{u}}^{k+1} - \boldsymbol{u}^k\right\|_0^2 + 2\Delta t\left(2\nu(\mathbf{D}\boldsymbol{u}^k)\mathbf{D}\widetilde{\boldsymbol{u}}^{k+1}, \mathbf{D}\widetilde{\boldsymbol{u}}^{k+1}\right) = 2\Delta t\left(\mathbf{f}^{k+1}, \widetilde{\boldsymbol{u}}^{k+1}\right),$$

and taking $\mathbf{v} = 2\Delta t \boldsymbol{u}^{k+1}$ in (8) gives

$$\begin{aligned} 0 &= \|\boldsymbol{u}^{k+1}\|_0^2 - \|\widetilde{\boldsymbol{u}}^{k+1}\|_0^2 + \|\boldsymbol{u}^{k+1} - \widetilde{\boldsymbol{u}}^{k+1}\|_0^2 + \Delta t \left(2\nu\left(\mathbf{D}\boldsymbol{u}^k\right)(\mathbf{D}\boldsymbol{u}^{k+1} - \mathbf{D}\widetilde{\boldsymbol{u}}^{k+1}), \mathbf{D}\boldsymbol{u}^{k+1} - \mathbf{D}\widetilde{\boldsymbol{u}}^{k+1}\right) + \\ & \quad \Delta t \left(2\nu\left(\mathbf{D}\boldsymbol{u}^k\right)\mathbf{D}\boldsymbol{u}^{k+1}, \mathbf{D}\boldsymbol{u}^{k+1}\right) - \Delta t \left(2\nu\left(\mathbf{D}\boldsymbol{u}^k\right)\mathbf{D}\widetilde{\boldsymbol{u}}^{k+1}, \mathbf{D}\widetilde{\boldsymbol{u}}^{k+1}\right). \end{aligned}$$

Summing the two equations yields

$$\begin{aligned} 2\Delta t(\mathbf{f}^{k+1}, \widetilde{\boldsymbol{u}}^{k+1}) &= \|\boldsymbol{u}^{k+1}\|_0^2 - \|\boldsymbol{u}^k\|_0^2 + \|\boldsymbol{u}^{k+1} - \widetilde{\boldsymbol{u}}^{k+1}\|_0^2 + \|\widetilde{\boldsymbol{u}}^{k+1} - \boldsymbol{u}^k\|_0^2 + \Delta t \left(2\nu\left(\mathbf{D}\boldsymbol{u}^k\right)\mathbf{D}\boldsymbol{u}^{k+1}, \mathbf{D}\boldsymbol{u}^{k+1}\right) + \\ & \quad \Delta t \left(2\nu\left(\mathbf{D}\boldsymbol{u}^k\right)(\mathbf{D}\boldsymbol{u}^{k+1} - \mathbf{D}\widetilde{\boldsymbol{u}}^{k+1}), \mathbf{D}\boldsymbol{u}^{k+1} - \mathbf{D}\widetilde{\boldsymbol{u}}^{k+1}\right) + \Delta t \left(2\nu\left(\mathbf{D}\boldsymbol{u}^k\right)\mathbf{D}\widetilde{\boldsymbol{u}}^{k+1}, \mathbf{D}\widetilde{\boldsymbol{u}}^{k+1}\right). \end{aligned}$$

Since $\nu\left(\mathbf{D}\boldsymbol{u}^k\right) \geq \nu_\infty$, then

$$\begin{aligned} 2\Delta t(\mathbf{f}^{k+1}, \widetilde{\boldsymbol{u}}^{k+1}) &\geq \|\boldsymbol{u}^{k+1}\|_0^2 - \|\boldsymbol{u}^k\|_0^2 + \|\boldsymbol{u}^{k+1} - \widetilde{\boldsymbol{u}}^{k+1}\|_0^2 + \|\widetilde{\mathbf{u}}^{k+1} - \boldsymbol{u}^k\|_0^2 + 2\nu_\infty \Delta t \left(\mathbf{D}\boldsymbol{u}^{k+1}, \mathbf{D}\boldsymbol{u}^{k+1}\right) + \\ & \quad 2\nu_\infty \Delta t \left(\mathbf{D}\boldsymbol{u}^{k+1} - \mathbf{D}\widetilde{\boldsymbol{u}}^{k+1}, \mathbf{D}\boldsymbol{u}^{k+1} - \mathbf{D}\widetilde{\boldsymbol{u}}^{k+1}\right) + 2\nu_\infty \Delta t \left(\mathbf{D}\widetilde{\boldsymbol{u}}^{k+1}, \mathbf{D}\widetilde{\boldsymbol{u}}^{k+1}\right). \end{aligned}$$

By virtue of the Korn's inequality, there exists a constant $C_r > 0$ such that

$$\begin{aligned} 2\Delta t(\mathbf{f}^{k+1}, \widetilde{\boldsymbol{u}}^{k+1}) &\geq \|\boldsymbol{u}^{k+1}\|_0^2 - \|\boldsymbol{u}^k\|_0^2 + \|\boldsymbol{u}^{k+1} - \widetilde{\boldsymbol{u}}^{k+1}\|_0^2 + \|\widetilde{\mathbf{u}}^{k+1} - \boldsymbol{u}^k\|_0^2 + 2C_r\nu_\infty \Delta t \|\nabla(\boldsymbol{u}^{k+1} - \widetilde{\boldsymbol{u}}^{k+1})\|_0^2 + \\ & \quad 2C_r\nu_\infty \Delta t \|\nabla \boldsymbol{u}^{k+1}\|_0^2 + 2C_r\nu_\infty \Delta t \|\nabla \widetilde{\boldsymbol{u}}^{k+1}\|_0^2. \end{aligned}$$

The left-hand side in the above inequality can be upper bounded by

$$2\Delta t(\mathbf{f}^{k+1}, \widetilde{\boldsymbol{u}}^{k+1}) \leq 2\Delta t \|\mathbf{f}^{k+1}\|_0 \|\widetilde{\boldsymbol{u}}^{k+1}\|_0 \leq \frac{\Delta t\, C_p^2}{2C_r\nu_\infty}\|\mathbf{f}^{k+1}\|_0^2 + 2C_r\nu_\infty \Delta t \|\nabla \widetilde{\boldsymbol{u}}^{k+1}\|_0^2,$$

which gives

$$\begin{aligned} \frac{\Delta t\, C_p^2}{2C\nu_\infty}\|\mathbf{f}^{k+1}\|_0^2 &\geq \|\boldsymbol{u}^{k+1}\|_0^2 - \|\boldsymbol{u}^k\|_0^2 + \|\boldsymbol{u}^{k+1} - \widetilde{\boldsymbol{u}}^{k+1}\|_0^2 + \|\widetilde{\mathbf{u}}^{k+1} - \boldsymbol{u}^k\|_0^2 + 2C_r\nu_\infty \Delta t \|\nabla(\boldsymbol{u}^{k+1} - \widetilde{\boldsymbol{u}}^{k+1})\|_0^2 + \\ & \quad 2C_r\nu_\infty \Delta t \|\nabla \boldsymbol{u}^{k+1}\|_0^2. \end{aligned}$$

performing the sum over $k = 0, 1, \ldots, K-1$ ends the proof. ■

Next we proceed to the demonstration of error estimates for both the velocity and the pressure in the appropriate norms, but first let us recall the following discrete Gronwall lemma [34] that will be repeatedly used in the next section:

Lemma 2.2. *For $k \in \mathbb{N}$, let κ and a_k, b_k, c_k, d_k be nonnegative numbers such that*

$$a_n + \Delta t \sum_{k=0}^{n} b_k \leq \kappa + \Delta t \sum_{k=0}^{n-1} a_k\, d_k + \Delta t \sum_{k=0}^{n-1} c_k, \qquad \forall n \geq 1.$$

Then, for all $n \geq 1$, the following inequality holds

$$a_n + \Delta t \sum_{k=0}^{n} b_k \leq \left(\kappa + \Delta t \sum_{k=0}^{n-1} c_k\right) \exp\left(\Delta t \sum_{k=0}^{n-1} d_k\right).$$

3. Error estimates for viscosity-splitting scheme

In this section we present error estimates for the approximation of $\boldsymbol{u}$ by the semi-discrete velocities $\widetilde{\boldsymbol{u}}^{k+1}$ and $\boldsymbol{u}^{k+1}$ in the norms $l^2\left(0,T;\mathbf{H}_0^1(\Omega)\right)$ and $l^\infty\left(0,T;\mathbf{L}^2(\Omega)\right)$, and the approximation of p by the semi-discrete pressure p^{k+1} in the norm $l^2\left(0,T;L^2(\Omega)\right)$. First, the approximations of $\boldsymbol{u}$ by $\widetilde{\boldsymbol{u}}^{k+1}$ and $\boldsymbol{u}^{k+1}$ in the norms $l^2\left(0,T;\mathbf{H}_0^1(\Omega)\right)$ and $l^\infty\left(0,T;\mathbf{L}^2(\Omega)\right)$ are estimated to be of order $1/2$, then this bound is improved to reach the order 1 provided that the solution of (1) enjoys sufficient regularity. Henceforth, $\boldsymbol{u}_0$ and $\mathbf{f}$ are assumed to satisfy the conditions

$$\boldsymbol{u}_0 \in \mathbf{H}^2(\Omega)\cap V, \qquad \mathbf{f}\in L^\infty\left(0,T;\mathbf{L}^2(\Omega)\right)\cap L^2\left(0,T;\mathbf{H}^1(\Omega)\right), \qquad \partial_t\mathbf{f}\in L^2\left(0,T;\mathbf{H}^{-1}(\Omega)\right), \tag{13}$$

in addition to the following properties of the solution $(\boldsymbol{u},p)$ of (1)

$$\sup_{t\in[0,T]}\left(\|\boldsymbol{u}(t,\cdot)\|_2 + \|\partial_t\boldsymbol{u}(t,\cdot)\|_1 + \|\partial_{tt}\boldsymbol{u}(t,\cdot)\|_{-1} + \|p(t,\cdot)\|_1\right) \le C, \tag{14}$$

where the subscripts t and tt stand for $\partial/\partial t$ and $\partial^2/\partial t^2$, respectively. Hereafter, (14) is assumed to be satisfied in addition to the following assumption

$$\boldsymbol{u}\in L^\infty\left([0,T],\mathbf{W}^{2,3+r}(\Omega)\right), \qquad r>0. \tag{15}$$

Note that the assumption (15) and the Sobolev injection from $\mathbf{W}^{1,3+r}(\Omega)$ into $\mathbf{L}^\infty(\Omega)$ (for $d=3$) ensure that there exists a constant $C_u>0$ such that

$$\sup_{t\in[0,T]}\|\mathbf{D}\boldsymbol{u}(t)\|_\infty \le C_u. \tag{16}$$

Let $\widetilde{\mathbf{e}}^{k+1}$ and $\mathbf{e}^{k+1}$ be respectively, the semi-discrete errors associated to $\widetilde{\boldsymbol{u}}^{k+1}$ and $\boldsymbol{u}^{k+1}$ defined by

$$\widetilde{\mathbf{e}}^{k+1} = \boldsymbol{u}(t_{k+1}) - \widetilde{\boldsymbol{u}}^{k+1}, \qquad \mathbf{e}^{k+1} = \boldsymbol{u}(t_{k+1}) - \boldsymbol{u}^{k+1},$$

the following lemma states a first estimates for the errors $\widetilde{\mathbf{e}}^{k+1}$ and $\mathbf{e}^{k+1}$, and it will be useful later to improve the error estimates.

Lemma 3.1. *Assume that* (14)-(16) *are satisfied and $m\le 1$. If in addition, the condition*

$$\frac{\nu_0}{\nu_\infty} \le 1 + \frac{\lambda_0}{\lambda}\,\frac{C_r}{5C_u}, \tag{17}$$

is satisfied, then

$$\left\|\mathbf{e}^{K+1}\right\|_0^2 + \|\widetilde{\mathbf{e}}^{K+1}\|_0^2 + \sum_{k=0}^{K}\left(\|\mathbf{e}^{k+1}-\widetilde{\mathbf{e}}^{k+1}\|_0^2 + \|\widetilde{\mathbf{e}}^{k+1}-\mathbf{e}^{k}\|_0^2\right) + 2C_r\nu_\infty\Delta t\sum_{k=0}^{K}\left(\left|\mathbf{e}^{k+1}\right|_1^2 + |\widetilde{\mathbf{e}}^{k+1}|_1^2 + |\mathbf{e}^{k+1}-\widetilde{\mathbf{e}}^{k+1}|_1^2\right) \le C\Delta t. \tag{18}$$

Proof. It should be stressed that the case with $m=1$ corresponds to Newtonian fluids and it is already addressed in [35] by tracing back the procedure adopted in [36]. The case with $m<1$ is treated following the same procedure.

Thus, writing (1) at time t_{k+1} and applying the Taylor's expansion with integral reminder, the truncation error denoted by $\mathbf{R}^k$ appears and it satisfies

$$\frac{\boldsymbol{u}(t_{k+1}) - \boldsymbol{u}(t_k)}{\Delta t} - \nabla\left(2\nu(\mathbf{D}\boldsymbol{u}(t_{k+1}))\mathbf{D}\boldsymbol{u}(t_{k+1})\right) + \boldsymbol{u}(t_{k+1}) \cdot \nabla\boldsymbol{u}(t_{k+1}) + \nabla p(t_{k+1}) = \mathbf{f}(t_{k+1}) + \mathbf{R}^k, \tag{19}$$

with

$$\mathbf{R}^k = \frac{1}{\Delta t}\int_{t_k}^{t_{k+1}} (t - t_k)\partial_{tt}\boldsymbol{u}(t)dt.$$

Here, the last expression is the residual integral of Taylor's expansion. Taking the inner product of (19) with $\mathbf{v} \in \mathbf{H}^1_0(\Omega)$ and subtracting (7) from it, yields

$$\frac{1}{\Delta t}\left(\widetilde{\mathbf{e}}^{k+1} - \mathbf{e}^k, \mathbf{v}\right) + \left(2\nu\left(\mathbf{D}\boldsymbol{u}(t_{k+1})\right)\mathbf{D}\boldsymbol{u}(t_{k+1}), \mathbf{D}\mathbf{v}\right) - \left(2\nu\left(\mathbf{D}\boldsymbol{u}^k\right)\mathbf{D}\widetilde{\boldsymbol{u}}^{k+1}, \mathbf{D}\mathbf{v}\right) = \left(\boldsymbol{u}^k \cdot \nabla\widetilde{\boldsymbol{u}}^{k+1}, \mathbf{v}\right) - \\ \left(\boldsymbol{u}(t_{k+1}) \cdot \nabla\boldsymbol{u}(t_{k+1}), \mathbf{v}\right) - \left(\nabla p(t_{k+1}), \mathbf{v}\right) + \langle\mathbf{R}^k, \mathbf{v}\rangle. \tag{20}$$

The last two terms in the left-hand side of (20) can be rewritten as

$$\left(2\nu\left(\mathbf{D}\boldsymbol{u}(t_{k+1})\right)\mathbf{D}\boldsymbol{u}(t_{k+1}), \mathbf{D}\mathbf{v}\right) - \left(2\nu\left(\mathbf{D}\boldsymbol{u}^k\right)\mathbf{D}\widetilde{\boldsymbol{u}}^{k+1}, \mathbf{D}\mathbf{v}\right) = \\ \left(\left(2\nu(\mathbf{D}\boldsymbol{u}(t_{k+1})) - 2\nu\left(\mathbf{D}\boldsymbol{u}^k\right)\right)\mathbf{D}\boldsymbol{u}(t_{k+1}), \mathbf{D}\mathbf{v}\right) + \left(2\nu\left(\mathbf{D}\boldsymbol{u}^k\right)\mathbf{D}\widetilde{\mathbf{e}}^{k+1}, \mathbf{D}\mathbf{v}\right),$$

while the non-linear terms in the right-hand side of (20) can be splitted up into three terms denoted respectively, by $B_1,\ B_2$ and B_3 as

$$\begin{aligned}\left(\boldsymbol{u}^k \cdot \nabla\widetilde{\boldsymbol{u}}^{k+1}, \mathbf{v}\right) - \left(\boldsymbol{u}(t_{k+1}) \cdot \nabla\boldsymbol{u}(t_{k+1}), \mathbf{v}\right) &= -\left(\mathbf{e}^k \cdot \nabla\widetilde{\boldsymbol{u}}^{k+1}, \mathbf{v}\right) + \left(\left(\boldsymbol{u}(t_k) - \boldsymbol{u}(t_{k+1})\right) \cdot \nabla\widetilde{\boldsymbol{u}}^{k+1}, \mathbf{v}\right) - \left(\boldsymbol{u}(t_{k+1}) \cdot \nabla\widetilde{\mathbf{e}}^{k+1}, \mathbf{v}\right), \\ &= B_1 + B_2 + B_3.\end{aligned}$$

Moreover, by choosing $\mathbf{v} = 2\Delta t\widetilde{\mathbf{e}}^{k+1}$, the term B_3 vanishes and (20) becomes

$$\|\widetilde{\mathbf{e}}^{k+1}\|_0^2 - \left\|\mathbf{e}^k\right\|_0^2 + \|\widetilde{\mathbf{e}}^{k+1} - \mathbf{e}^k\|_0^2 + 2\Delta t\left(2\nu\left(\mathbf{D}\boldsymbol{u}^k\right)\mathbf{D}\widetilde{\mathbf{e}}^{k+1}, \mathbf{D}\widetilde{\mathbf{e}}^{k+1}\right) = 2\Delta t\langle\mathbf{R}, \widetilde{\mathbf{e}}^{k+1}\rangle - 2\Delta t\left(\nabla p(t_{k+1}), \widetilde{\mathbf{e}}^{k+1}\right) - \\ 2\Delta t\left(\left(2\nu(\mathbf{D}\boldsymbol{u}(t_{k+1})) - 2\nu\left(\mathbf{D}\boldsymbol{u}^k\right)\right)\mathbf{D}\boldsymbol{u}(t_{k+1}), \mathbf{D}\widetilde{\mathbf{e}}^{k+1}\right) + 2\Delta t B_1 + 2\Delta t B_2. \tag{21}$$

The first equation in (8) with the choice of $\mathbf{v} = 2\Delta t\mathbf{e}^{k+1}$ can be reformulated as follows

$$\|\mathbf{e}^{k+1}\|_0^2 - \|\widetilde{\mathbf{e}}^{k+1}\|_0^2 + \|\mathbf{e}^{k+1} - \widetilde{\mathbf{e}}^{k+1}\|_0^2 + \Delta t\left(2\nu\left(\mathbf{D}\boldsymbol{u}^k\right)\mathbf{D}\mathbf{e}^{k+1}, \mathbf{D}\mathbf{e}^{k+1}\right) + \\ \Delta t\left(2\nu\left(\mathbf{D}\boldsymbol{u}^k\right)\mathbf{D}\left(\mathbf{e}^{k+1} - \widetilde{\mathbf{e}}^{k+1}\right), \mathbf{D}\left(\mathbf{e}^{k+1} - \widetilde{\mathbf{e}}^{k+1}\right)\right) - \Delta t\left(2\nu\left(\mathbf{D}\boldsymbol{u}^k\right)\mathbf{D}\widetilde{\mathbf{e}}^{k+1}, \mathbf{D}\widetilde{\mathbf{e}}^{k+1}\right) = 0. \tag{22}$$

Adding the last equation to (21) results in

$$\|\mathbf{e}^{k+1}\|_0^2 - \left\|\mathbf{e}^k\right\|_0^2 + \|\mathbf{e}^{k+1} - \widetilde{\mathbf{e}}^{k+1}\|_0^2 + \|\widetilde{\mathbf{e}}^{k+1} - \mathbf{e}^k\|_0^2 + \Delta t\left(2\nu\left(\mathbf{D}\boldsymbol{u}^k\right)\mathbf{D}\widetilde{\mathbf{e}}^{k+1}, \mathbf{D}\widetilde{\mathbf{e}}^{k+1}\right) + \\ \Delta t\left(2\nu\left(\mathbf{D}\boldsymbol{u}^k\right)\mathbf{D}\mathbf{e}^{k+1}, \mathbf{D}\mathbf{e}^{k+1}\right) + \Delta t\left(2\nu\left(\mathbf{D}\boldsymbol{u}^k\right)\mathbf{D}\left(\mathbf{e}^{k+1} - \widetilde{\mathbf{e}}^{k+1}\right), \mathbf{D}\left(\mathbf{e}^{k+1} - \widetilde{\mathbf{e}}^{k+1}\right)\right) = \\ 2\Delta t\langle\mathbf{R}, \widetilde{\mathbf{e}}^{k+1}\rangle - 2\Delta t\left(\nabla p(t_{k+1}), \widetilde{\mathbf{e}}^{k+1}\right) - 2\Delta t\left(\left(2\nu(\mathbf{D}\boldsymbol{u}(t_{k+1})) - 2\nu\left(\mathbf{D}\boldsymbol{u}^k\right)\right)\mathbf{D}\boldsymbol{u}(t_{k+1}), \mathbf{D}\widetilde{\mathbf{e}}^{k+1}\right) + 2\Delta t(B_1 + B_2).$$

Since $\nu\left(\mathbf{D}\boldsymbol{u}^k\right) \geq \nu_\infty$ and $\nu(\mathbf{D}\boldsymbol{u}(t_{k+1})) \geq \nu_\infty$, and by virtue of the Korn's inequality, the viscosity terms in the left-hand side of the last equation can be lower bounded as follows

$$\begin{aligned}
2C_r\nu_\infty\Delta t|\widetilde{\mathbf{e}}^{k+1}|_1^2 &\leq \Delta t\left(2\nu\left(\mathbf{D}\boldsymbol{u}^k\right)\mathbf{D}\widetilde{\mathbf{e}}^{k+1}, \mathbf{D}\widetilde{\mathbf{e}}^{k+1}\right),\\
2C_r\nu_\infty\Delta t\left|\mathbf{e}^{k+1}\right|_1^2 &\leq \Delta t\left(2\nu\left(\mathbf{D}\boldsymbol{u}^k\right)\mathbf{D}\mathbf{e}^{k+1}, \mathbf{D}\mathbf{e}^{k+1}\right),\\
2C_r\nu_\infty\Delta t|\mathbf{e}^{k+1}-\widetilde{\mathbf{e}}^{k+1}|_1^2 &\leq \Delta t\left(2\nu\left(\mathbf{D}\boldsymbol{u}^k\right)\mathbf{D}\left(\mathbf{e}^{k+1}-\widetilde{\mathbf{e}}^{k+1}\right), \mathbf{D}\left(\mathbf{e}^{k+1}-\widetilde{\mathbf{e}}^{k+1}\right)\right),
\end{aligned}$$

which leads to

$$\begin{aligned}
&\|\mathbf{e}^{k+1}\|_0^2 - \left\|\mathbf{e}^k\right\|_0^2 + \|\mathbf{e}^{k+1}-\widetilde{\mathbf{e}}^{k+1}\|_0^2 + \|\widetilde{\mathbf{e}}^{k+1}-\mathbf{e}^k\|_0^2 + 2C_r\nu_\infty\Delta t|\widetilde{\mathbf{e}}^{k+1}|_1^2 + 2C_r\nu_\infty\Delta t\left|\mathbf{e}^{k+1}\right|_1^2 + 2C_r\nu_\infty\Delta t|\mathbf{e}^{k+1}-\widetilde{\mathbf{e}}^{k+1}|_1^2\\
&\quad\leq 2\Delta t\langle\mathbf{R}, \widetilde{\mathbf{e}}^{k+1}\rangle - 2\Delta t\left(\nabla p(t_{k+1}), \widetilde{\mathbf{e}}^{k+1}\right) - 2\Delta t\left(\left(2\nu(\mathbf{D}\boldsymbol{u}(t_{k+1})) - 2\nu\left(\mathbf{D}\boldsymbol{u}^k\right)\right)\mathbf{D}\boldsymbol{u}(t_{k+1}), \mathbf{D}\widetilde{\mathbf{e}}^{k+1}\right) + \\
&\quad 2\Delta t B_1 + 2\Delta t B_2.
\end{aligned}\tag{23}$$

The terms in the right-hand side of (23) are bounded as follows

- The integral residual term:

$$\begin{aligned}
2\Delta t\langle\mathbf{R}, \widetilde{\mathbf{e}}^{k+1}\rangle &\leq 2\Delta t\|\mathbf{R}^k\|_{-1}|\widetilde{\mathbf{e}}^{k+1}|_1,\\
&\leq \frac{2C_r\nu_\infty}{10}\Delta t|\widetilde{\mathbf{e}}^{k+1}|_1^2 + C\Delta t\|\mathbf{R}^k\|_{-1}^2 = \frac{2C_r\nu_\infty}{10}\Delta t|\widetilde{\mathbf{e}}^{k+1}|_1^2 + \frac{C}{\Delta t}\|\int_{t_k}^{t_{k+1}}(t-t_k)\partial_{tt}\boldsymbol{u}(t)dt\|_{-1}^2,\\
&\leq \frac{2C_r\nu_\infty}{10}\Delta t|\widetilde{\mathbf{e}}^{k+1}|_1^2 + \frac{C}{\Delta t}\int_{t_k}^{t_{k+1}}\|\partial_{tt}\boldsymbol{u}\|_{-1}^2 dt\int_{t_k}^{t_{k+1}}(t-t_k)^2 dt,\\
&\leq \frac{2C_r\nu_\infty}{10}\Delta t|\widetilde{\mathbf{e}}^{k+1}|_1^2 + C(\Delta t)^2\int_{t_k}^{t_{k+1}}\|\partial_{tt}\boldsymbol{u}\|_{-1}^2 dt.
\end{aligned}\tag{24}$$

- The pressure term: since $\nabla\cdot\mathbf{e}^k = 0$, we have

$$2\Delta t\left(\nabla p(t_{k+1}), \widetilde{\mathbf{e}}^{k+1}\right) = 2\Delta t\left(\nabla p(t_{k+1}), \widetilde{\mathbf{e}}^{k+1}-\mathbf{e}^k\right),$$

  which can be upper bounded by

$$\begin{aligned}
2\Delta t\left(\nabla p(t_{k+1}), \widetilde{\mathbf{e}}^{k+1}\right) &= 2\Delta t\left(\nabla p(t_{k+1}), \widetilde{\mathbf{e}}^{k+1}-\mathbf{e}^k\right),\\
&\leq 2\Delta t\|\nabla p(t_{k+1})\|_0\|\widetilde{\mathbf{e}}^{k+1}-\mathbf{e}^k\|_0,\\
&\leq 2(\Delta t)^2\|\nabla p(t_{k+1})\|_0^2 + \frac{1}{2}\|\widetilde{\mathbf{e}}^{k+1}-\mathbf{e}^k\|_0^2.
\end{aligned}$$

- Since $m < 1$ and under the assumption (16),

$$\begin{aligned}
-2\Delta t\left(\left(2\nu(\mathbf{D}\boldsymbol{u}(t_{k+1})) - 2\nu\left(\mathbf{D}\boldsymbol{u}^k\right)\right)\mathbf{D}\boldsymbol{u}(t_{k+1}), \mathbf{D}\widetilde{\mathbf{e}}^{k+1}\right) \leq C(\Delta t)^2\int_{t_k}^{t_{k+1}}|\partial_t\boldsymbol{u}|_1^2\,dt + \frac{20C_u^2C_\nu^2}{C_r\nu_\infty}\Delta t|\mathbf{e}^k|_1^2 +\\
\frac{4C_r\nu_\infty}{10}\Delta t|\widetilde{\mathbf{e}}^{k+1}|_1^2.
\end{aligned}\tag{25}$$

  The complete proof of this estimate is detailed in Appendix A.

- The non-linear terms $2\Delta t B_1$ and $2\Delta t B_2$: using the continuity properties and the skew-symmetry of the trilinear form c and (14), we obtain

$$\begin{aligned}
2\Delta t B_1 &= -2\Delta t\left(\mathbf{e}^k\cdot\nabla\widetilde{\boldsymbol{u}}^{k+1},\widetilde{\mathbf{e}}^{k+1}\right),\\
&= -2\Delta t\left(\mathbf{e}^k\cdot\nabla\boldsymbol{u}(t_{k+1}),\widetilde{\mathbf{e}}^{k+1}\right),\\
&\le 2C\Delta t\left\|\mathbf{e}^k\right\|_0\|\boldsymbol{u}(t_{k+1})\|_2|\widetilde{\mathbf{e}}^{k+1}|_1,\\
&\le \frac{2C_r\nu_\infty}{10}\Delta t|\widetilde{\mathbf{e}}^{k+1}|_1^2+C\Delta t\left\|\mathbf{e}^k\right\|_0^2,
\end{aligned}$$

and

$$\begin{aligned}
2\Delta t B_2 &= 2\Delta t\left((\boldsymbol{u}(t_k)-\boldsymbol{u}(t_{k+1}))\cdot\nabla\widetilde{\boldsymbol{u}}^{k+1},\widetilde{\mathbf{e}}^{k+1}\right),\\
&= 2\Delta t\left((\boldsymbol{u}(t_k)-\boldsymbol{u}(t_{k+1}))\cdot\nabla\boldsymbol{u}(t_{k+1}),\widetilde{\mathbf{e}}^{k+1}\right),\\
&\le 2\Delta t\|\boldsymbol{u}(t_k)-\boldsymbol{u}(t_{k+1})\|_0\|\boldsymbol{u}(t_{k+1})\|_2|\widetilde{\mathbf{e}}^{k+1}|_1,\\
&\le 2C\Delta t|\widetilde{\mathbf{e}}^{k+1}|_1\|\int_{t_k}^{t_{k+1}}\partial_t\boldsymbol{u}(t)dt\|_0,\\
&\le 2C\Delta t|\widetilde{\mathbf{e}}^{k+1}|_1\sqrt{\Delta t}\left(\int_{t_k}^{t_{k+1}}\|\partial_t\boldsymbol{u}\|_0^2dt\right)^{1/2},\\
&\le \frac{2C_r\nu_\infty}{10}\Delta t|\widetilde{\mathbf{e}}^{k+1}|_1^2+C(\Delta t)^2\int_{t_k}^{t_{k+1}}\|\partial_t\boldsymbol{u}\|_0^2dt.
\end{aligned}$$

Using all theses inequalities, (23) becomes

$$\begin{aligned}
\|\mathbf{e}^{k+1}\|_0^2-\left\|\mathbf{e}^k\right\|_0^2+\|\mathbf{e}^{k+1}-\widetilde{\mathbf{e}}^{k+1}\|_0^2+\frac{1}{2}\|\widetilde{\mathbf{e}}^{k+1}-\mathbf{e}^k\|_0^2+2C_r\nu_\infty\Delta t\left(\frac{1}{2}|\widetilde{\mathbf{e}}^{k+1}|_1^2+\left|\mathbf{e}^{k+1}\right|_1^2+|\mathbf{e}^{k+1}-\widetilde{\mathbf{e}}^{k+1}|_1^2\right)\le\\
C(\Delta t)^2\int_{t_k}^{t_{k+1}}\|\partial_{tt}\boldsymbol{u}\|_{-1}^2dt+2(\Delta t)^2\|\nabla p(t_{k+1})\|_0^2+C(\Delta t)^2\int_{t_k}^{t_{k+1}}|\partial_t\boldsymbol{u}|_1^2\,dt+\\
\frac{20C_u^2C_\nu^2}{C_r\nu_\infty}\Delta t|\mathbf{e}^k|_1^2+C(\Delta t)^2\int_{t_k}^{t_{k+1}}\|\partial_t\boldsymbol{u}\|_0^2dt+C\Delta t\left\|\mathbf{e}^k\right\|_0^2.
\end{aligned}$$

Taking the sum over $k=0,1,\ldots,K$ and using (14), we get

$$\begin{aligned}
&\|\mathbf{e}^{K+1}\|_0^2+\sum_{k=0}^K\left(\|\mathbf{e}^{k+1}-\widetilde{\mathbf{e}}^{k+1}\|_0^2+\frac{1}{2}\|\widetilde{\mathbf{e}}^{k+1}-\mathbf{e}^k\|_0^2\right)+2C_r\nu_\infty\Delta t\sum_{k=0}^K\left(\frac{1}{2}|\widetilde{\mathbf{e}}^{k+1}|_1^2+\left|\mathbf{e}^{k+1}\right|_1^2+|\mathbf{e}^{k+1}-\widetilde{\mathbf{e}}^{k+1}|_1^2\right)\le\\
&C\Delta t\left(\Delta t\int_0^T\|\partial_{tt}\boldsymbol{u}\|_{-1}^2dt+\sup_{t\in[0,T]}\|\nabla p(t)\|_0^2+\Delta t\int_0^T|\partial_t\boldsymbol{u}|_1^2\,dt+\Delta t\int_0^T\|\partial_t\boldsymbol{u}\|_0^2dt+\sum_{k=0}^K\left\|\mathbf{e}^k\right\|_0^2\right)+\frac{20C_u^2C_\nu^2}{C_r\nu_\infty}\Delta t\sum_{k=0}^K|\mathbf{e}^k|_1^2\le\\
&C\Delta t+C\Delta t\sum_{k=0}^K\left\|\mathbf{e}^k\right\|_0^2+\frac{20C_u^2C_\nu^2}{C_r\nu_\infty}\Delta t\sum_{k=0}^K|\mathbf{e}^k|_1^2.
\end{aligned}$$

By virtue of the assumption (17), we can take the last term in the right-hand side to the other side of the inequality and then apply the discrete Gronwall lemma to obtain

$$\left\|\mathbf{e}^{K+1}\right\|_0^2+C_r\nu_\infty\Delta t|\mathbf{e}^{K+1}|_1^2+\sum_{k=0}^K\left(\|\mathbf{e}^{k+1}-\widetilde{\mathbf{e}}^{k+1}\|_0^2+\|\widetilde{\mathbf{e}}^{k+1}-\mathbf{e}^k\|_0^2\right)+2C_r\nu_\infty\Delta t\sum_{k=0}^K\left(\frac{1}{2}|\mathbf{e}^{k+1}|_1^2+\frac{1}{2}|\widetilde{\mathbf{e}}^{k+1}|_1^2+|\mathbf{e}^{k+1}-\widetilde{\mathbf{e}}^{k+1}|_1^2\right)\le C\Delta t,$$

which yields

$$\left\|\mathbf{e}^{K+1}\right\|_0^2 \ + \ \sum_{k=0}^{K}\left(\|\mathbf{e}^{k+1}-\widetilde{\mathbf{e}}^{k+1}\|_0^2+\|\widetilde{\mathbf{e}}^{k+1}-\mathbf{e}^{k}\|_0^2\right) \ + \ 2C_r\nu_\infty\Delta t\sum_{k=0}^{K}\left(|\mathbf{e}^{k+1}|_1^2+|\widetilde{\mathbf{e}}^{k+1}|_1^2+|\mathbf{e}^{k+1}-\widetilde{\mathbf{e}}^{k+1}|_1^2\right) \quad \leq \quad C\Delta t. \quad (26)$$

Finally, by using (26) we bound the term $\|\widetilde{\mathbf{e}}^{K+1}\|_0^2$ as follows

$$\begin{aligned}\|\widetilde{\mathbf{e}}^{K+1}\|_0^2 \quad &\leq \quad 2\left(\|\mathbf{e}^{K+1}-\widetilde{\mathbf{e}}^{K+1}\|_0^2+\left\|\mathbf{e}^{K+1}\right\|_0^2\right),\\ &\leq \quad C\Delta t,\end{aligned}$$

and (18) is proved. ■

Note that Lemma 3.1 yields a 1/2 order estimates for the velocity errors in the norms $l^\infty\left(0,T;\mathbf{L}^2(\Omega)\right)$ and $l^2\left(0,T;\mathbf{H}_0^1(\Omega)\right)$. The next lemma improves these results to reach the first-order estimate. Unlike the standard projection schemes this improvement can be obtained without using the Stokes operator, thanks to the boundary condition on $\boldsymbol{u}^{k+1}$ in (8).

Lemma 3.2. *Under the assumptions* (14)*,* (16)*,* (17) *and $m \leq 1$, we have for small enough Δt*

$$\left\|\mathbf{e}^{K+1}\right\|_0^2+\sum_{k=0}^{K}\left\|\mathbf{e}^{k+1}-\mathbf{e}^{k}\right\|_0^2+C_r\nu_\infty\Delta t\sum_{k=0}^{K}\left|\mathbf{e}^{k+1}\right|_1^2 \quad \leq \quad C(\Delta t)^2, \quad (27)$$

$$\Delta t\sum_{k=0}^{K}\|p(t_{k+1})-p^{k+1}\|_0^2 \quad \leq \quad C\Delta t. \quad (28)$$

Proof. Taking the inner product of (19) with $\mathbf{v}\in\mathbf{H}_0^1(\Omega)$ gives

$$\frac{1}{\Delta t}\left(\boldsymbol{u}(t_{k+1})-\boldsymbol{u}(t_k),\mathbf{v}\right)+\left(2\nu(\mathbf{D}\boldsymbol{u}(t_{k+1}))\mathbf{D}\boldsymbol{u}(t_{k+1}),\mathbf{D}\mathbf{v}\right)+\left(\boldsymbol{u}(t_{k+1})\cdot\nabla\boldsymbol{u}(t_{k+1}),\mathbf{v}\right)+\left(\nabla p(t_{k+1}),\mathbf{v}\right)=$$
$$\left(\mathbf{f}(t_{k+1}),\mathbf{v}\right)+\langle\mathbf{R}^k,\mathbf{v}\rangle. \quad (29)$$

Adding (7) to (8) and subtracting the sum from (29) yields

$$\frac{1}{\Delta t}\left(\mathbf{e}^{k+1}-\mathbf{e}^{k},\mathbf{v}\right)+\left(2\nu\left(\mathbf{D}\boldsymbol{u}(t_{k+1})\right)\mathbf{D}\boldsymbol{u}(t_{k+1}),\mathbf{D}\mathbf{v}\right)-\left(2\nu\left(\mathbf{D}\boldsymbol{u}^k\right)\mathbf{D}\boldsymbol{u}^{k+1},\mathbf{D}\mathbf{v}\right)=$$
$$\left(\boldsymbol{u}^k\cdot\nabla\widetilde{\boldsymbol{u}}^{k+1},\mathbf{v}\right)-\left(\boldsymbol{u}(t_{k+1})\cdot\nabla\boldsymbol{u}(t_{k+1}),\mathbf{v}\right)+\langle\mathbf{R}^k,\mathbf{v}\rangle+\left(\nabla p^{k+1},\mathbf{v}\right)-\left(\nabla p(t_{k+1}),\mathbf{v}\right). \quad (30)$$

By choosing $\mathbf{v}=2\Delta t\mathbf{e}^{k+1}$ in the last equation, we get

$$\|\mathbf{e}^{k+1}\|_0^2-\left\|\mathbf{e}^{k}\right\|_0^2+\left\|\mathbf{e}^{k+1}-\mathbf{e}^{k}\right\|_0^2+2\Delta t\left(2\nu\left(\mathbf{D}\boldsymbol{u}(t_{k+1})\right)\mathbf{D}\boldsymbol{u}(t_{k+1}),\mathbf{D}\mathbf{e}^{k+1}\right)-2\Delta t\left(2\nu\left(\mathbf{D}\boldsymbol{u}^k\right)\mathbf{D}\boldsymbol{u}^{k+1},\mathbf{D}\mathbf{e}^{k+1}\right)=$$
$$2\Delta t\left(\boldsymbol{u}^k\cdot\nabla\widetilde{\boldsymbol{u}}^{k+1},\mathbf{e}^{k+1}\right)-2\Delta t\left(\boldsymbol{u}(t_{k+1})\cdot\nabla\boldsymbol{u}(t_{k+1}),\mathbf{e}^{k+1}\right)+2\Delta t\langle\mathbf{R}^k,\mathbf{e}^{k+1}\rangle.$$

Next, we rewrite the viscous terms as

$$2\Delta t\left(2\nu\left(\mathbf{D}\boldsymbol{u}(t_{k+1})\right)\mathbf{D}\boldsymbol{u}(t_{k+1}),\mathbf{D}\mathbf{e}^{k+1}\right)-2\Delta t\left(2\nu\left(\mathbf{D}\boldsymbol{u}^k\right)\mathbf{D}\boldsymbol{u}^{k+1},\mathbf{D}\mathbf{e}^{k+1}\right)=$$
$$2\Delta t\left(\left(2\nu\left(\mathbf{D}\boldsymbol{u}(t_{k+1})\right)-2\nu\left(\mathbf{D}\boldsymbol{u}^k\right)\right)\mathbf{D}\boldsymbol{u}(t_{k+1}),\mathbf{D}\mathbf{e}^{k+1}\right)+2\Delta t\left(2\nu\left(\mathbf{D}\boldsymbol{u}^k\right)\mathbf{D}\mathbf{e}^{k+1},\mathbf{D}\mathbf{e}^{k+1}\right),$$

and using the lower bound of the viscosity ν and the Korn's inequality we have

$$\|\mathbf{e}^{k+1}\|_0^2 - \left\|\mathbf{e}^k\right\|_0^2 + \left\|\mathbf{e}^{k+1} - \mathbf{e}^k\right\|_0^2 + 2C_r\nu_\infty\Delta t\left|\mathbf{e}^{k+1}\right|_1^2 \leq 2\Delta t\langle\mathbf{R}^k, \mathbf{e}^{k+1}\rangle + 2\Delta t\left(\boldsymbol{u}^k\cdot\nabla\widetilde{\boldsymbol{u}}^{k+1}, \mathbf{e}^{k+1}\right) - 2\Delta t\left(\boldsymbol{u}(t_{k+1})\cdot\nabla\boldsymbol{u}(t_{k+1}), \mathbf{e}^{k+1}\right) - 2\Delta t\left(\left(2\nu\left(\mathbf{D}\boldsymbol{u}(t_{k+1})\right) - 2\nu(\mathbf{D}\boldsymbol{u}^k\right))\mathbf{D}\boldsymbol{u}(t_{k+1}), \mathbf{D}\mathbf{e}^{k+1}\right). \quad (31)$$

Next, we bound each term in the right-hand side of (31) as follow: The integral residual term is treated in a similar way as for (24) yielding

$$\begin{aligned} 2\Delta t\langle\mathbf{R}^k, \mathbf{e}^{k+1}\rangle &\leq 2\Delta t\|\mathbf{R}^k\|_{-1}\left|\mathbf{e}^{k+1}\right|_1, \\ &\leq \frac{C_r\nu_\infty}{7}\Delta t\left|\mathbf{e}^{k+1}\right|_1^2 + C(\Delta t)^2\int_{t_k}^{t_{k+1}}\|\partial_{tt}\boldsymbol{u}\|_{-1}^2\,dt. \end{aligned}$$

The non-linear terms are splitted into

$$\begin{aligned} &2\Delta t\left(\boldsymbol{u}^k\cdot\nabla\widetilde{\boldsymbol{u}}^{k+1}, \mathbf{e}^{k+1}\right) - 2\Delta t\left(\boldsymbol{u}(t_{k+1})\cdot\nabla\boldsymbol{u}(t_{k+1}), \mathbf{e}^{k+1}\right) = \\ &\quad - 2\Delta t\left(\boldsymbol{u}(t_{k+1})\cdot\nabla\widetilde{\mathbf{e}}^{k+1}, \mathbf{e}^{k+1}\right) - 2\Delta t\left(\left(\boldsymbol{u}(t_{k+1}) - \boldsymbol{u}(t_k)\right)\cdot\nabla\widetilde{\boldsymbol{u}}^{k+1}, \mathbf{e}^{k+1}\right) - 2\Delta t\left(\mathbf{e}^k\cdot\nabla\widetilde{\boldsymbol{u}}^{k+1}, \mathbf{e}^{k+1}\right) = \\ &\quad - 2\Delta t\left(\boldsymbol{u}(t_{k+1})\cdot\nabla\widetilde{\mathbf{e}}^{k+1}, \mathbf{e}^{k+1}\right) - 2\Delta t\left(\left(\boldsymbol{u}(t_{k+1}) - \boldsymbol{u}(t_k)\right)\cdot\nabla\widetilde{\boldsymbol{u}}^{k+1}, \mathbf{e}^{k+1}\right) + 2\Delta t\left(\mathbf{e}^k\cdot\nabla\widetilde{\mathbf{e}}^{k+1}, \mathbf{e}^{k+1}\right) - \\ &\quad\quad 2\Delta t\left(\mathbf{e}^k\cdot\nabla\boldsymbol{u}(t_{k+1}), \mathbf{e}^{k+1}\right). \end{aligned}$$

Using (14), (10) and the results from Lemma 3.1, we have

$$\begin{aligned} -2\Delta t\left(\boldsymbol{u}(t_{k+1})\cdot\nabla\widetilde{\mathbf{e}}^{k+1}, \mathbf{e}^{k+1}\right) &\leq C\Delta t\|\boldsymbol{u}(t_{k+1})\|_2\|\widetilde{\mathbf{e}}^{k+1}\|_0\left|\mathbf{e}^{k+1}\right|_1, \\ &\leq \frac{C_r\nu_\infty}{7}\Delta t\left|\mathbf{e}^{k+1}\right|_1^2 + C\Delta t\|\widetilde{\mathbf{e}}^{k+1}\|_0^2, \end{aligned}$$

and

$$\begin{aligned} -2\Delta t\left(\left(\boldsymbol{u}(t_{k+1}) - \boldsymbol{u}(t_k)\right)\cdot\nabla\widetilde{\boldsymbol{u}}^{k+1}, \mathbf{e}^{k+1}\right) &\leq C\Delta t|\boldsymbol{u}(t_{k+1}) - \boldsymbol{u}(t_k)|_1|\widetilde{\boldsymbol{u}}^{k+1}|_1\left|\mathbf{e}^{k+1}\right|_1, \\ &\leq \frac{C_r\nu_\infty}{7}\Delta t\left|\mathbf{e}^{k+1}\right|_1^2 + C(\Delta t)^2\int_{t_k}^{t_{k+1}}|\partial_t\boldsymbol{u}|_1^2\,dt, \end{aligned}$$

where we have used the bound

$$\exists\, C > 0, \quad |\widetilde{\boldsymbol{u}}^{k+1}|_1 \leq C, \qquad \forall\, k = 0, 1, \ldots, K,$$

that follows from Lemma 3.1 and assumption (14) by simply writing

$$|\widetilde{\boldsymbol{u}}^{k+1}|_1 \leq |\widetilde{\mathbf{e}}^{k+1}|_1 + |\boldsymbol{u}(t_{k+1})|_1.$$

Thus, from (10) and Lemma 3.1 we have,

$$\begin{aligned} 2\Delta t\left(\mathbf{e}^k\cdot\nabla\widetilde{\mathbf{e}}^{k+1}, \mathbf{e}^{k+1}\right) &\leq C\Delta t|\mathbf{e}^k|_1\left|\mathbf{e}^{k+1}\right|_1\|\widetilde{\mathbf{e}}^{k+1}\|_0^{1/2}|\widetilde{\mathbf{e}}^{k+1}|_1^{1/2}, \\ &\leq C(\Delta t)^{5/4}|\mathbf{e}^k|_1\left|\mathbf{e}^{k+1}\right|_1, \\ &\leq \frac{C_r\nu_\infty}{7}\Delta t\left|\mathbf{e}^{k+1}\right|_1^2 + C(\Delta t)^{3/2}|\mathbf{e}^k|_1^2, \end{aligned}$$

and

$$
\begin{aligned}
-2\Delta t\left(\mathbf{e}^k\cdot\nabla\boldsymbol{u}(t_{k+1}),\mathbf{e}^{k+1}\right) &\le C\Delta t\left\|\mathbf{e}^k\right\|_0\|\boldsymbol{u}(t_{k+1})\|_2\left|\mathbf{e}^{k+1}\right|_1,\\
&\le \frac{C_r\nu_\infty}{7}\Delta t\left|\mathbf{e}^{k+1}\right|_1^2+C\Delta t\left\|\mathbf{e}^k\right\|_0^2.
\end{aligned}
$$

The last term in the right-hand side of (31) can be treated the same way as detailed in Appendix A to get

$$
-2\Delta t\left(\left(2\nu\left(\mathbf{D}\boldsymbol{u}(t_{k+1})\right)-2\nu(\mathbf{D}\boldsymbol{u}^k)\right)\mathbf{D}\boldsymbol{u}(t_{k+1}),\mathbf{D}\mathbf{e}^{k+1}\right)\le C(\Delta t)^2\int_{t_k}^{t_{k+1}}|\partial_t\boldsymbol{u}|_1^2\,dt+\frac{28C_u^2C_\nu^2}{C_r\nu_\infty}\Delta t|\mathbf{e}^k|_1^2+\frac{2C_r\nu_\infty}{7}\Delta t\left|\mathbf{e}^{k+1}\right|_1^2.
$$

Considering the established inequalities and taking the sum over $k=0,1,\dots,K$, (31) becomes

$$
\begin{aligned}
\left\|\mathbf{e}^{K+1}\right\|_0^2+\sum_{k=0}^{K}\left\|\mathbf{e}^{k+1}-\mathbf{e}^k\right\|_0^2+C_r\nu_\infty\Delta t\sum_{k=0}^{K}\left|\mathbf{e}^{k+1}\right|_1^2 &\le C(\Delta t)^2\int_0^T\|\partial_{tt}\boldsymbol{u}\|_{-1}^2dt+C\Delta t\sum_{k=0}^{K}\|\widetilde{\mathbf{e}}^{k+1}\|_0^2+\\
&C(\Delta t)^2\int_0^T|\partial_t\boldsymbol{u}|_1^2\,dt+C(\Delta t)^{3/2}\sum_{k=0}^{K}|\mathbf{e}^k|_1^2+\frac{28C_u^2C_\nu^2}{C_r\nu_\infty}\Delta t\sum_{k=0}^{K}|\mathbf{e}^k|_1^2+C\Delta t\sum_{k=0}^{K}\left\|\mathbf{e}^k\right\|_0^2.
\end{aligned}
$$

Using (14), we deduce

$$
\begin{aligned}
\left\|\mathbf{e}^{K+1}\right\|_0^2+\sum_{k=0}^{K}\left\|\mathbf{e}^{k+1}-\mathbf{e}^k\right\|_0^2+C_r\nu_\infty\Delta t\sum_{k=0}^{K}\left|\mathbf{e}^{k+1}\right|_1^2 &\le C(\Delta t)^2+C\Delta t\sum_{k=0}^{K}\|\widetilde{\mathbf{e}}^{k+1}\|_0^2+\\
&C(\Delta t)^{3/2}\sum_{k=0}^{K}|\mathbf{e}^k|_1^2+\frac{28C_u^2C_\nu^2}{C_r\nu_\infty}\Delta t\sum_{k=0}^{K}|\mathbf{e}^k|_1^2+C\Delta t\sum_{k=0}^{K}\left\|\mathbf{e}^k\right\|_0^2.
\end{aligned}
$$

Writing

$$
\left\|\widetilde{\mathbf{e}}^{k+1}\right\|_0^2\le 2\left(\|\widetilde{\mathbf{e}}^{k+1}-\mathbf{e}^{k+1}\|_0^2+\|\mathbf{e}^{k+1}\|_0^2\right),
$$

and using the estimates in Lemma 3.1, we obtain

$$
\left\|\mathbf{e}^{K+1}\right\|_0^2+\sum_{k=0}^{K}\left\|\mathbf{e}^{k+1}-\mathbf{e}^k\right\|_0^2+C_r\nu_\infty\Delta t\sum_{k=0}^{K}\left|\mathbf{e}^{k+1}\right|_1^2\le C(\Delta t)^2+C\Delta t\sum_{k=0}^{K}\|\mathbf{e}^{k+1}\|_0^2+C(\Delta t)^{3/2}\sum_{k=0}^{K}|\mathbf{e}^k|_1^2+\frac{28C_u^2C_\nu^2}{C_r\nu_\infty}\Delta t\sum_{k=0}^{K}|\mathbf{e}^k|_1^2.
$$

For small enough Δt we can write

$$
C(\Delta t)^{3/2}\sum_{k=0}^{K}|\mathbf{e}^k|_1^2\le\frac{28C_u^2C_\nu^2}{C_r\nu_\infty}\Delta t\sum_{k=0}^{K}|\mathbf{e}^k|_1^2.
$$

Hence,

$$
\left\|\mathbf{e}^{K+1}\right\|_0^2+\sum_{k=0}^{K}\left\|\mathbf{e}^{k+1}-\mathbf{e}^k\right\|_0^2+C_r\nu_\infty\Delta t\sum_{k=0}^{K}\left|\mathbf{e}^{k+1}\right|_1^2\le C(\Delta t)^2+C\Delta t\sum_{k=0}^{K}\|\mathbf{e}^{k+1}\|_0^2+\frac{56C_u^2C_\nu^2}{C_r\nu_\infty}\Delta t\sum_{k=0}^{K}|\mathbf{e}^k|_1^2.
$$

Taking into account (17) we get

$$
\left\|\mathbf{e}^{K+1}\right\|_0^2+\frac{1}{2}C_r\nu_\infty\Delta t|\mathbf{e}^{K+1}|_1^2+\sum_{k=0}^{K}\left\|\mathbf{e}^{k+1}-\mathbf{e}^k\right\|_0^2+\frac{1}{2}C_r\nu_\infty\Delta t\sum_{k=0}^{K}\left|\mathbf{e}^{k+1}\right|_1^2\le C(\Delta t)^2+C\Delta t\sum_{k=0}^{K}\|\mathbf{e}^{k+1}\|_0^2.
$$

Applying the Gronwall lemma to the last inequality gives

$$
\left\|\mathbf{e}^{K+1}\right\|_0^2+\sum_{k=0}^{K}\left\|\mathbf{e}^{k+1}-\mathbf{e}^k\right\|_0^2+C_r\nu_\infty\Delta t\sum_{k=0}^{K}\left|\mathbf{e}^{k+1}\right|_1^2\le C(\Delta t)^2.
$$

Finally, the estimate (28) can be obtained combining Appendix A and the same arguments used in [35] for the Newtonian fluid flows.

■

It should be stressed that using the same arguments as those reported in [37, 38, 30], we can easily improve the error estimates (27) and (28) by stating the following lemma for which we omit its proof:

Lemma 3.3. *Under the assumptions of Lemma 3.2. If the continuous solution has the following additional regularity*

$$\sqrt{t}\,\partial_{tt}\boldsymbol{u} \in L^2\left(0, T; \mathbf{L}^2(\Omega)\right) \quad \textit{and} \quad \partial_{ttt}\boldsymbol{u} \in L^2\left(0, T; \mathbf{V}'\right). \tag{32}$$

Then

$$\begin{aligned} \left\|\mathbf{e}^{k+1}\right\|_{\ell^\infty(\mathbf{L}^2)\cap\ell^2(\mathbf{H}^1)} + \left\|\tilde{\mathbf{e}}^{k+1}\right\|_{\ell^\infty(\mathbf{L}^2)\cap\ell^2(\mathbf{H}^1_{loc})} &\leq C\Delta t \\ \left\|p(t^{k+1}) - p^{k+1}\right\|_{\ell^2(L^2)} &\leq C\Delta t. \end{aligned} \tag{33}$$

Note that based on the above estimates, the error in the pressure approximation reaches a full first-order accuracy in $l^2\left(0, T_f; L^2(\Omega)\right)$. This is also supported by the numerical results illustrated in the next section.

4. Numerical results

We examine the performance of the viscosity-splitting method for solving two examples of non-Newtonian fluid flows governed by the equations (1)-(4) in both two and three space dimensions. For the spatial discretization, we employ the well-established Taylor-Hood $\mathbb{P}_2/\mathbb{P}_1$ mixed finite elements. Here, the quadratic $\mathbb{P}_2$ finite elements are used for the velocity field $\boldsymbol{u}$ whereas the linear $\mathbb{P}_1$ finite elements are used for the pressure solution p. In all our computations the resulting linear systems of algebraic equations in (7)-(8) were solved using a preconditioned Generalized Minimal Residual (GMRES) iterative solver. We used the diagonal as a preconditioner and a tolerance of 10^{-7} to stop the iterations. Here, we used the Freefem++ software [39] for the implementation of the considered viscosity-splitting method.

4.1. Accuracy example

We first consider an accuracy test example by solving the equations (1)-(4) with a manufactured analytical solution. The computational domain is assumed to be an unit cuboid domain $\Omega = [0, 1] \times [0, 1] \times [0, 1]$ subject to homogeneous Dirichlet-type boundary conditions and the source function $\mathbf{f}$ is defined such that the exact solution of (1)-(4) is given by

$$\begin{aligned} \boldsymbol{u}(t, x, y, z) &= \left(x + x^2 + xy + xz, y + y^2 - xy - 3yz, -2z + z^2 - xz - 3yz\right)^\top (1 - \cos(t)), \\ p(t, x, y, z) &= (x - y + z)(1 - \cos(t)). \end{aligned}$$

We consider the Carreau constitutive relation (4) with

$$\nu_\infty = 0.01, \qquad \nu_0 = 1, \qquad \lambda_0 = 1, \qquad \lambda = 1.$$

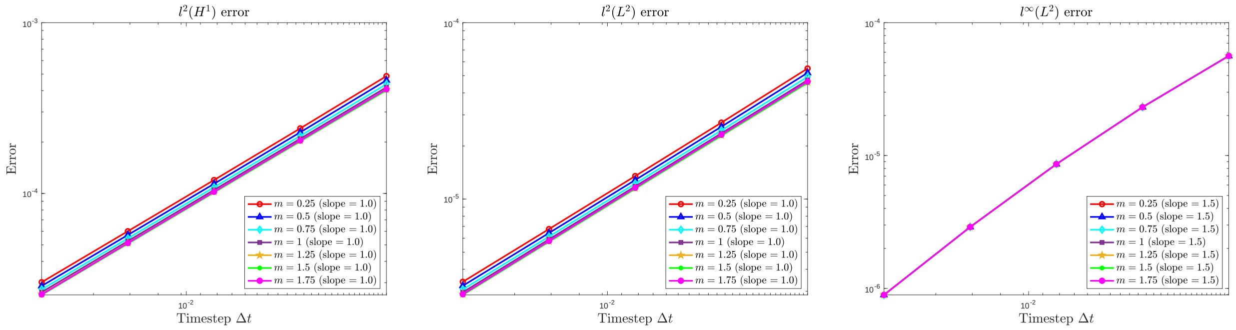

Figure 1: Convergence results obtained for the velocity solution in the accuracy example using different fluid cases.

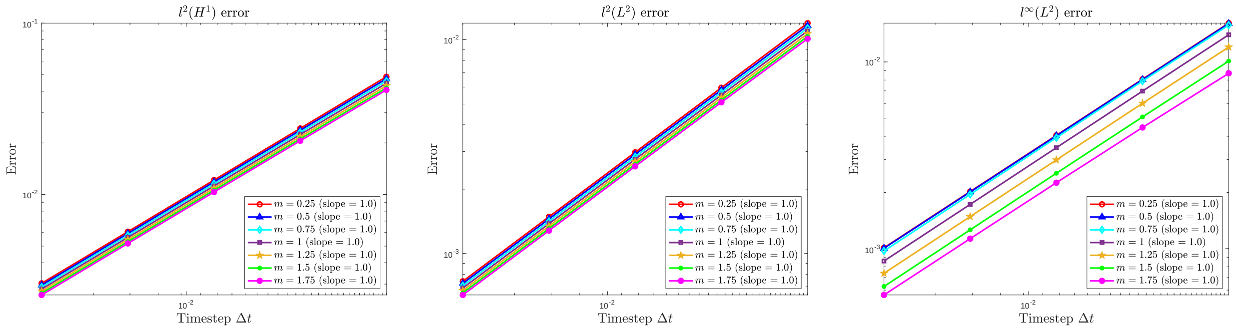

Figure 2: Convergence results obtained for the pressure solution in the accuracy example using different fluid cases.

To evaluate the convergence of the viscosity-splitting method, we calculate the errors between the numerical and analytical solutions using the following norms

$$||\mathbf{e}||_{l^2(X)} = \left(\Delta t \sum_{k=0}^{K} ||\mathbf{e}^k||_X^2\right)^{1/2}, \qquad ||\mathbf{e}||_{l^\infty(X)} = \underset{k=0,1,\ldots,K}{sup} ||\mathbf{e}^k||_X,$$

where X is taken as $\left(L^2(\Omega)\right)^3$ or $\left(H^1(\Omega)\right)^3$ for the velocity solution, and as $L^2(\Omega)$ or $H^1(\Omega)$ for the pressure solution. Here, the simulations are performed using different time steps defined by $\Delta t = \dfrac{0.1}{2^j}$ $(j = 1, \ldots, 5)$ and the results are presented at the final time $t = 0.5$. A structured finite element mesh with $20\times20\times20$ elements is used in this example.

In Figure 1 we present the convergence plots obtained for the velocity field using the considered norms and different values of the parameter m in the constitutive law (4) namely $m = 0.25$, 0.5, 0.75, 1, 1.25, 1.5 and 1.75 which correspond to different classes of the fluid under study. Those convergence plots obtained for the pressure solution are illustrated in Figure 2. For the considered test cases, it is clear that the method is first-order for the velocity approximation in the norms $l^2\left(0, T; \boldsymbol{L}^2(\Omega)\right)$, $l^2\left(0, T; \boldsymbol{H}^1(\Omega)\right)$ and $l^\infty\left(0, T; \boldsymbol{L}^2(\Omega)\right)$. In addition, this convergence order is also maintained regardless of the fluid class *i.e.* Newtonian ($m = 1$), shear-thinning ($m < 1$) or shear-thickening ($m > 1$), but with a slight change in the error magnitude depending on the value of the power index m. Here, the

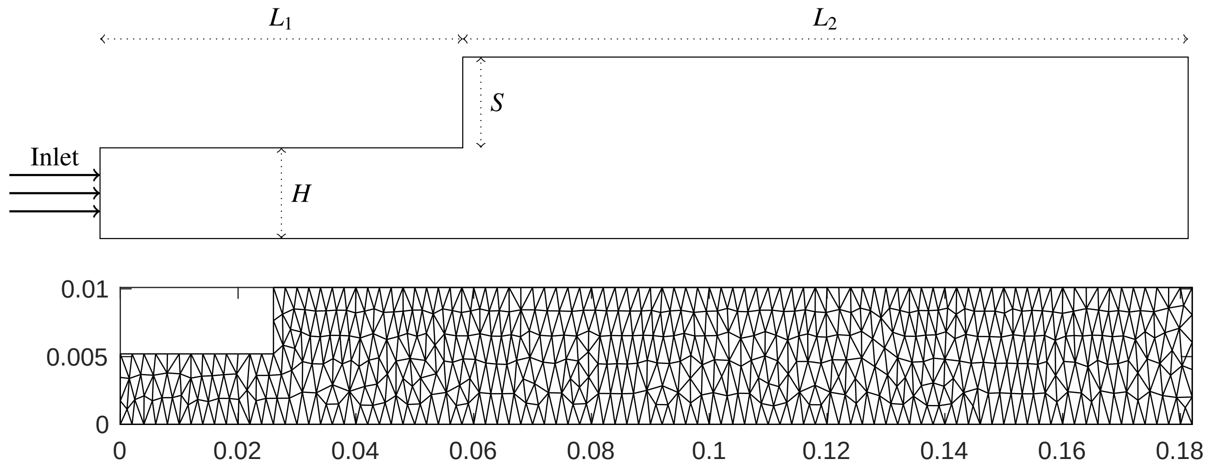

Figure 3: Configuration of the computational domain (top plot) and the unstructured mesh used in simulations for $Re = 400$ (bottom plot).

error decreases as the fluid changes from the shear-thinning case ($m < 1$) to the shear-thickening case ($m > 1$). For the results obtained for the pressure approximation in Figure 2, a full first-order rate can clearly be seen in these convergence plots for the selected flow conditions. For the considered test cases, we obviously notice that the error plots keep the same trend which is also consistent with the error estimates proved in the present study.

4.2. Forward-facing step flow

In this test example, we apply the viscosity-splitting method for solving the two-dimensional benchmark problem of forward-facing step flow for which the mathematical governing equations are given by (1)-(4). Following for example [40], the computational domain is of height $H = 5.2\ mm$, length before the step $L_1 = 26\ mm$, height of the step $S = 4.9\ mm$, and length after the step $L_2 = 156\ mm$ as shown in Figure 3. Here, the fluid enters the domain from the inlet face with a constant velocity u_0, for which the Reynolds number is defined by $Re = \rho u_0(2H)/\nu_\infty$. The velocity boundary conditions for the step geometry include the no-slip velocity for all solid walls, a parabolic velocity profile at the inlet, and zero normal stress at the outlet. As in the previous example, we use the Carreau constitutive relation (4) with

$$\nu_\infty = 0.0035\ Pa.s, \qquad \nu_0 = 0.25\ Pa.s, \qquad \lambda_0 = 1, \qquad \lambda = 25\ s \qquad m = 0.25.$$

It should be noted that this step is similar to the one adopted in [40] for solving Newtonian and non-Newtonian fluid flows using a variational multiscale method. Notice that in the Newtonian case ($m = 1$), the viscosity is set to $\nu_\infty = \nu_0 = 0.00345\ Pa.s$. To reduce the computational cost in our simulations, we have adopted the mesh adaptation procedure proposed in [39] such that we locally refine or de-refine the mesh based on the quality of solutions after every 100 time steps. Figure 3 depicts the initial computational mesh used in the simulations for the selected flow

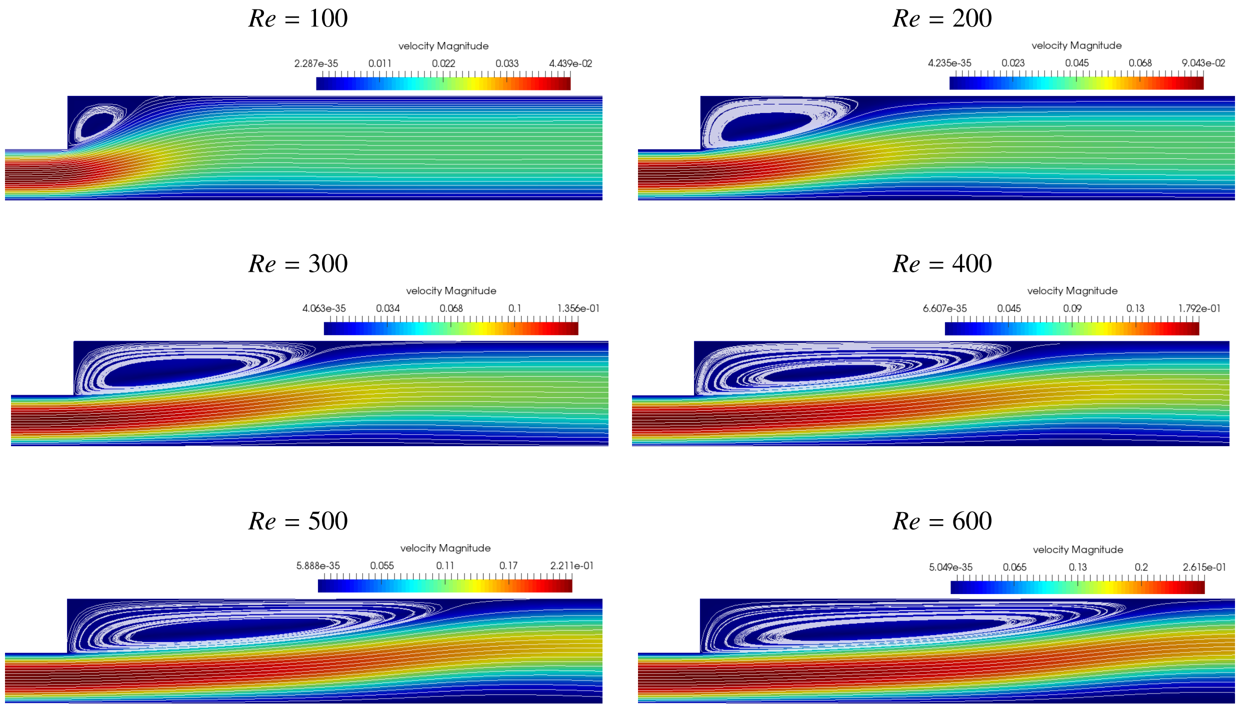

Figure 4: Velocity magnitudes and streamlines obtained for the forward-facing step flow at six different Reynolds numbers.

regimes. Here, the unstructured mesh contains 904 elements with 549 pressure nodes and 2001 velocity nodes. The time step Δt is fixed to 0.02 and steady-state solutions are presented. In all results presented in this section, the time loop was terminated when the relative difference between two consecutive computed solutions in L^2-norm is less than a tolerance of 10^{-6}.

Figure 4 displays snapshots of the velocity magnitude along with the streamlines obtained using six different Reynolds numbers, namely Re = 100, 200, 300, 400, 500 and 600. From these results, we can see that the size of the recirculation zone and the position of the reattachment point become large as the Reynolds number Re increases. Indeed, at low Reynolds numbers, the inertial effects are less intense particularly near the step walls (mainly due to the viscosity effects) and consequently the fluid near the step walls can not resist the adverse pressure gradient created by the sudden expansion after the step. Therefore, losses in the core flow occur as shown by the velocity magnitude right after crossing the step, while near the step walls the flow is completely reversed creating a small recirculation zone. This shear-thinning fluid behavior is expected to resemble the Newtonian case since at low shear-rates with $m < 1$, the Carreau model tends towards a viscosity of Newtonian fluids. On the other hand, as the Reynolds number increases, the inertial effects become stronger with larger velocity gradients near the step walls which reduce the viscous effects (shear-thinning) and the fluid is pushed for a longer distance downstream against the retarding pressure force making a progressively stretched recirculation area. These results are in good agreement with those reported in [40] where

Table 1: Results for the length of recirculation zone obtained for the forward-facing step flow at six different Reynolds numbers.

	Re = 100	Re = 200	Re = 300	Re = 400	Re = 500	Re = 600
Current work	1.4746	3.0344	4.5144	6.0696	7.4129	8.3408
Results from [40]	1.4136	3.1099	4.7435	6.2932	NA	NA

authors performed similar simulations using a variational multiscale method. To further quantify the performance of the viscosity-splitting method, we compute the normalized length of the recirculation zone x/H for the considered Reynolds numbers and the obtained results are summarized in Table 1. Again, compared to the method studied in [40], our results are in good agreement and indicate that the recirculation region for a shear-thinning fluid gets enlarged as the Reynolds number Re increases which is also supported by the velocity magnitude and streamlines in Figure 4. Although not studied here, the shear-thickening case is expected to have an opposite behavior due to the fact that larger shear rates would enhance the viscosity and consequently more energy dissipation occurs near the step [40]. It is also worth remarking that the main part of the computational work in the solution procedure was devoted to the linear solver used to solve the linear systems of algebraic equations associated with the viscosity-splitting scheme (7)-(8). For all the results presented in this section, the number of iterations to reach the tolerance of 10^{-7} does not exceed 65 iterations for the considered Reynolds numbers. Needless to mention that the viscosity-splitting algorithm presented in the current work can be highly optimized for vector computers, because it does not require non-linear solvers and contain no recursive elements. Some difficulties may arise from the fact that for efficient vectorization the data should be stored continuously within long vectors rather than two- or three-dimensional arrays.

As a final remark we would like to comment on the computational costs for the proposed viscosity-splitting scheme and its monolithic counterpart applied to this example of non-Newtonian fluid flows. To this end we summarize in Table 2 the CPU times required for each method solving the forward-facing step flow at four different Reynolds numbers using $m = 0.25$ and $m = 0.5$. It is clear that for a fixed Reynolds number, the CPU time increases as the power index m decreases in both methods but the proposed viscosity-splitting scheme is far more efficient than its monolithic counterpart for all selected Reynolds numbers. Unlike the monolithic approach for which the CPU time increases as the Reynolds number increases, the CPU time in the viscosity-splitting scheme decreases as the Reynolds number increases. Under the considered flow conditions for this test example, the viscosity-splitting scheme is more efficient than the monolithic approach. For instance at $Re = 600$, the viscosity-splitting scheme is more than 9 times faster than its monolithic counterpart for both power indices $m = 0.25$ and $m = 0.5$. This is mainly attributed to the computational work required for solving the Stokes problems which have different structures in the monolithic and viscosity-splitting algorithms. Here, non-symmetric linear systems are obtained in the monolithic algorithm and in the first step of the viscosity-splitting algorithm while the linear system in the second step of the viscosity-splitting

Table 2: CPU times (in minutes) obtained for the forward-facing step flow at four different Reynolds numbers using the standrad monolithic and the proposed viscosity-splitting methods with $m = 0.25$ and $m = 0.5$.

	$m = 0.25$				$m = 0.5$			
	$Re = 100$	$Re = 200$	$Re = 400$	$Re = 600$	$Re = 100$	$Re = 200$	$Re = 400$	$Re = 600$
Monolithic	176.8	178.8	260.8	353.7	150.4	169.5	242.5	346.1
Viscosity-splitting	46.8	38.9	36.7	36.0	44.6	39.8	39.0	37.3

algorithm is symmetric. This later linear system can be efficiently solved using for example the conjugate gradient solver. It should also be pointed out that most of the computational effort goes into solving the linear systems in the viscosity-splitting algorithm. Therefore, reducing the computational cost in the viscosity-splitting method can be achieved by implementing a more efficient preconditioned iterative solver for these linear systems. For instance, multigrid techniques are well known to be among most efficient methods for solving linear systems and can therefore be the suitable tools to increase the efficiency of the viscosity-splitting method. Needless to say, the CPU time in the proposed viscosity-splitting method can be drastically reduced if parallel computers were used in the simulations.

5. Conclusions

In this work, we have studied the error estimates of a viscosity-splitting scheme in time applied to non-Newtonian fluid flows. The governing equations consist of the incompressible Navier-Stokes equations with a non-linear viscosity depending on the shear-rate magnitude according to a generic model. The main difficulty in establishing error estimates for this class of generalized Newtonian fluids lies in the additional terms that appear due to the fact that the viscosity is no longer a constant quantity but non-linearly depends on the shear-rate. These terms could have degraded the theoretical estimates, therefore they required a proper treatment with extra assumptions on the exact solution as well as the parameters inherited in the fluid model. The considered time stepping consists of splitting the convection term and incompressibility constraint into two separate time steps. In contrast to the well-established projection methods, the viscosity in the present method is not dropped in the last step allowing to enforce the full original boundary conditions on the end-of-step velocity which eliminates any concerns about the numerical boundary layers. We have established first-order error estimates for both the velocity solution in both $\boldsymbol{L}^1$- and $\boldsymbol{H}^1$-norms, and for the pressure solution in the L^2-norm. To demonstrate the performance of the viscosity-splitting scheme, numerical results obtained for an example with known exact solution and for the benchmark of forward-facing flow problem are assessed. The obtained results for both examples exhibit good numerical convergence and confirm the established theoretical estimates. In future work, we will focus on establishing high-order estimates in the viscosity-splitting scheme by using, for example, the second-order implicit backward differentiation formula. Extension of this analysis to generalized thermal Newtonian fluids with more complicated constitutive laws is also considered for future work.

Declaration of competing interest

The authors declare that they have no known competing financial interests or personal relationships that could have appeared to influence the work reported in this paper.

Data availability

The data that support the findings of this study are available from the corresponding author upon reasonable request.

Acknowledgment

The authors would like to thank anonymous referees for giving very helpful comments and suggestions that have greatly improved this paper.

Appendix A.

In this appendix, we detail the estimate (25) by defining its left-hand term as

$$I = -2\Delta t\left(\left(2\nu(\mathbf{D}\boldsymbol{u}(t_{k+1})) - 2\nu\left(\mathbf{D}\boldsymbol{u}^k\right)\right)\mathbf{D}\boldsymbol{u}(t_{k+1}), \mathbf{D}\widetilde{\mathbf{e}}^{k+1}\right). \tag{A.1}$$

Let G be the mapping defined by

$$\begin{aligned} G : \mathbb{R}^{d\times d} &\longrightarrow \mathbb{R} \\ \mathbf{s} &\longmapsto \nu_\infty + (\nu_0 - \nu_\infty)\left(\lambda_0 + \lambda^2 \|\mathbf{s}\|^2\right)^\alpha \end{aligned}$$

where $\alpha = \frac{m-1}{2}$, $m < 1$. Hence, its differential is given by

$$dG_{\mathbf{s}}(\mathbf{h}) = 2\alpha\lambda^2(\nu_0 - \nu_\infty)\left(\lambda_0 + \lambda^2\|\mathbf{s}\|^2\right)^{\alpha-1}\langle \mathbf{s}, \mathbf{h}\rangle, \qquad \forall\, \mathbf{h} \in \mathbb{R}^{d\times d}.$$

The norm of $dG_{\mathbf{s}}$ is bounded by

$$\|dG_{\mathbf{s}}\| \leq 2|\alpha|\lambda^2(\nu_0 - \nu_\infty)\left(\lambda_0 + \lambda^2\|\mathbf{s}\|^2\right)^{\alpha-1}\|\mathbf{s}\|.$$

Let us denote by g the real function

$$g(t) = 2|\alpha|\lambda^2(\nu_0 - \nu_\infty)\left(\lambda_0 + \lambda^2 t^2\right)^{\alpha-1} t, \qquad \forall t \in \mathbb{R}.$$

By taking the derivative of g with respect to t, it can be shown that g is bounded on $\mathbb{R}_+$. Hence, there exists a constant C_ν such that

$$\sup_{\mathbf{s}\in\mathbb{R}^{d\times d},\mathbf{s}\neq 0} \frac{\|dG_{\mathbf{s}}\|}{\|\mathbf{s}\|} \leq C_\nu$$

where

$$C_\nu = 2|\alpha|\lambda\,(\nu_0 - \nu_\infty)\left(\frac{2(1-\alpha)\lambda_0}{1-2\alpha}\right)^{\alpha-1} \frac{\sqrt{\lambda_0}}{\sqrt{1-2\alpha}}.$$

Consequently, the mean-value theorem (see for instance [41]) gives

$$|G(\mathbf{s}_1) - G(\mathbf{s}_2)| \leq C_\nu\,\|\mathbf{s}_1 - \mathbf{s}_2\|\,, \qquad \forall\,\mathbf{s}_1,\mathbf{s}_2 \in \mathbb{R}^{d\times d}. \tag{A.2}$$

Thus,

$$\begin{aligned}
I &\leq 2\Delta t \int_\Omega \left|2\nu(\mathbf{D}\boldsymbol{u}(t_{k+1})) - 2\nu\left(\mathbf{D}\boldsymbol{u}^k\right)\right| \left|\mathbf{D}\boldsymbol{u}(t_{k+1}) : \mathbf{D}\widetilde{\mathbf{e}}^{k+1}\right|\,dx, \qquad \text{(using Cauchy-Schwarz's inequality)},\\
&\leq 4\Delta t\left(\int_\Omega |\nu(\mathbf{D}\boldsymbol{u}(t_{k+1})) - \nu\left(\mathbf{D}\boldsymbol{u}^k\right)|^2\,\|\mathbf{D}\boldsymbol{u}(t_{k+1})\|^2\,dx\right)^{1/2} \left\|\mathbf{D}\widetilde{\mathbf{e}}^{k+1}\right\|_0, \qquad \text{(by assumption (16))},\\
&\leq 4\Delta t\,C_u\left(\int_\Omega |\nu(\mathbf{D}\boldsymbol{u}(t_{k+1})) - \nu\left(\mathbf{D}\boldsymbol{u}^k\right)|^2\,dx\right)^{1/2} \left\|\mathbf{D}\widetilde{\mathbf{e}}^{k+1}\right\|_0, \qquad \text{(using (A.2))},\\
&\leq 4\Delta t\,C_uC_\nu\left(\int_\Omega \|\mathbf{D}\boldsymbol{u}(t_{k+1}) - \mathbf{D}\boldsymbol{u}^k\|^2\,dx\right)^{1/2} \left\|\mathbf{D}\widetilde{\mathbf{e}}^{k+1}\right\|_0,\\
&\leq 4\Delta t C_uC_\nu\|\mathbf{D}\boldsymbol{u}(t_{k+1}) - \mathbf{D}\boldsymbol{u}(t_k)\|_0 \left\|\mathbf{D}\widetilde{\mathbf{e}}^{k+1}\right\|_0 + 4\Delta t C_uC_\nu\|\mathbf{D}\boldsymbol{u}(t_k) - \mathbf{D}\boldsymbol{u}^k\|_0 \left\|\mathbf{D}\widetilde{\mathbf{e}}^{k+1}\right\|_0,\\
&= J_1 + J_2,
\end{aligned}$$

where J_1 and J_2 denote the last two terms in the right-hand side, respectively. These terms can be upper bounded as

$$\begin{aligned}
J_1 &\leq C\Delta t|\boldsymbol{u}(t_{k+1}) - \boldsymbol{u}(t_k)|_1\left|\widetilde{\mathbf{e}}^{k+1}\right|_1 = C\Delta t\left|\int_{t_k}^{t_{k+1}} \partial_t\boldsymbol{u}\,dt\right|_1 \left|\widetilde{\mathbf{e}}^{k+1}\right|_1,\\
&\leq C(\Delta t)^{3/2}\left(\int_{t_k}^{t_{k+1}} |\partial_t\boldsymbol{u}|_1^2\,dt\right)^{1/2} \left|\widetilde{\mathbf{e}}^{k+1}\right|_1,\\
&\leq C(\Delta t)^2\int_{t_k}^{t_{k+1}} |\partial_t\boldsymbol{u}|_1^2\,dt + \frac{2C_r\nu_\infty}{10}\Delta t\left|\widetilde{\mathbf{e}}^{k+1}\right|_1^2,
\end{aligned}$$

and

$$\begin{aligned}
J_2 &= 4\Delta t C_uC_\nu\|\mathbf{D}\boldsymbol{u}(t_k) - \mathbf{D}\boldsymbol{u}^k\|_0\left\|\mathbf{D}\widetilde{\mathbf{e}}^{k+1}\right\|_0 = 4\Delta t C_uC_\nu\|\mathbf{D}\mathbf{e}^k\|_0\left\|\mathbf{D}\widetilde{\mathbf{e}}^{k+1}\right\|_0,\\
&\leq \frac{20C_u^2C_\nu^2}{C_r\nu_\infty}\Delta t\|\mathbf{D}\mathbf{e}^k\|_0^2 + \frac{2C_r\nu_\infty}{10}\Delta t\left\|\mathbf{D}\widetilde{\mathbf{e}}^{k+1}\right\|_0^2,\\
&\leq \frac{20C_u^2C_\nu^2}{C_r\nu_\infty}\Delta t|\mathbf{e}^k|_1^2 + \frac{2C_r\nu_\infty}{10}\Delta t|\widetilde{\mathbf{e}}^{k+1}|_1^2.
\end{aligned}$$

Hence, the term I is upper bounded by

$$I \leq C(\Delta t)^2\int_{t_k}^{t_{k+1}} |\partial_t\boldsymbol{u}|_1^2\,dt + \frac{20C_u^2C_\nu^2}{C_r\nu_\infty}\Delta t|\mathbf{e}^k|_1^2 + \frac{4C_r\nu_\infty}{10}\Delta t|\widetilde{\mathbf{e}}^{k+1}|_1^2. \tag{A.3}$$

References

[1] R. Chhabra, J. Richardson, Non-newtonian flow and applied rheology: Engineering applications second edition preface to first edition, Non-Newtonian Flow and Applied Rheology: Engineering Applications, (2008).

[2] M. M. Cross, Rheology of non-newtonian fluids: a new flow equation for pseudoplastic systems, Journal of colloid science 20 (5) (1965) 417–437.

[3] F. Irgens, Rheology and non-newtonian fluids, Vol. 1, Springer, 2014.

[4] A. Ibarz, G. V. Barbosa-Cánovas, Unit operations in food engineering, CRC press, 2002.

[5] A. J. Chorin, Numerical solution of the navier-stokes equations, Mathematics of computation 22 (104) (1968) 745–762.

[6] R. Temam, Sur l'approximation de la solution des équations de navier-stokes par la méthode des pas fractionnaires (ii), Archive for rational mechanics and analysis 33 (1969) 377–385.

[7] K. Goda, A multistep technique with implicit difference schemes for calculating two-or three-dimensional cavity flows, Journal of computational physics 30 (1) (1979) 76–95.

[8] L. J. Timmermans, P. D. Minev, F. N. Van De Vosse, An approximate projection scheme for incompressible flow using spectral elements, International journal for numerical methods in fluids 22 (7) (1996) 673–688.

[9] J. Guermond, J. Shen, On the error estimates for the rotational pressure-correction projection methods, Mathematics of Computation 73 (248) (2004) 1719–1737.

[10] J.-L. Guermond, P. Minev, J. Shen, Error analysis of pressure-correction schemes for the time-dependent stokes equations with open boundary conditions, SIAM Journal on Numerical Analysis 43 (1) (2005) 239–258.

[11] G. Karniadakis, M. Israeli, S. Orszag, High-order splitting methods for the incompressible navier-stokes equations, Journal of Computational Physics 97 (2) (1991) 414 – 443.

[12] S. A. Orszag, M. Israeli, M. O. Deville, Boundary conditions for incompressible flows, Journal of Scientific Computing 1 (1986) 75–111.

[13] J. Blasco, R. Codina, A. Huerta, A fractional-step method for the incompressible navier–stokes equations related to a predictor–multicorrector algorithm, International Journal for Numerical Methods in Fluids 28 (10) (1998) 1391–1419.

[14] J. Deteix, D. Yakoubi, Improving the pressure accuracy in a projection scheme for incompressible fluids with variable viscosity, Applied Mathematics Letters 79 (2018) 111–117.

[15] L. Plasman, J. Deteix, D. Yakoubi, A projection scheme for navier-stokes with variable viscosity and natural boundary condition, International Journal for Numerical Methods in Fluids 92 (12) (2020) 1845–1865.

[16] D. R. Pacheco, R. Schussnig, T.-P. Fries, An efficient split-step framework for non-newtonian incompressible flow problems with consistent pressure boundary conditions, Computer Methods in Applied Mechanics and Engineering 382 (2021) 113888.

[17] J. Liu, Open and traction boundary conditions for the incompressible navier–stokes equations, Journal of Computational Physics 228 (19) (2009) 7250–7267.

[18] A. Amani, A. Naseri, C. D. Pérez-Segarra, A. Oliva, A method for fluid-structure interaction problems with non-newtonian fluid, in: Proceedings of the 6th European Conference on Computational Mechanics (Solids, Structures and Coupled Problems) and the 7th European Conference on Computational Fluid Dynamics, Glasgow, UK, 2018, pp. 101–110.

[19] J. Deteix, D. Yakoubi, Shear rate projection schemes for non-newtonian fluids, Computer Methods in Applied Mechanics and Engineering 354 (2019) 620–636.

[20] W. Gao, R. Liu, A hybrid finite volume/finite element method for incompressible generalized newtonian fluid flows on unstructured triangular meshes, Acta Mechanica Sinica 25 (6) (2009) 747.

[21] G. D. Ilio, D. Chiappini, G. Bella, A comparison of numerical methods for non-newtonian fluid flows in a sudden expansion, International Journal of Modern Physics C 27 (12) (2016) 1650139.

[22] M. Jabbari, J. McDonough, E. Mitsoulis, J. H. Hattel, Application of a projection method for simulating flow of a shear-thinning fluid, Fluids 4 (3) (2019) 124.

[23] H.-O. Bae, J. Wolf, Sufficient conditions for local regularity to the generalized Newtonian fluid with shear thinning viscosity, Zeitschrift für angewandte Mathematik und Physik 68 (1) (2016) 7.

[24] Z. Tan, J. Zhou, Partial regularity of a certain class of non-Newtonian fluids, Journal of Mathematical Analysis and Applications 455 (2) (2017) 1529 – 1558.

[25] P. Dreyfuss, N. Hungerbühler, Results on a Navier-Stokes system with applications to electrorheological fluid flow, Int. J. Pure Appl. Math. 14 (2) (2004) 241–271.

[26] H.-O. Bae, Regularity criterion for generalized Newtonian fluids in bounded domains, Journal of Mathematical Analysis and Applications 421 (1) (2015) 489 – 500.

[27] L. Diening, M. Růžička, J. Wolf, Existence of weak solutions for unsteady motions of generalized Newtonian fluids, Ann. Sc. Norm. Super. Pisa Cl. Sci. (5) 9 (1) (2010) 1–46.

[28] J.-L. Guermond, P. Minev, J. Shen, An overview of projection methods for incompressible flows, Computer methods in applied mechanics and engineering 195 (44-47) (2006) 6011–6045.

[29] R. Temam, Navier-Stokes equations: theory and numerical analysis, Vol. 343, American Mathematical Soc., 2001.

[30] D. Yakoubi, Enhancing the viscosity-splitting method to solve the time-dependent Navier-Stokes equations, Commun. Nonlinear Sci. Numer. Simul. 123 (2023) 17, id/No 107264.

[31] P. Constantin, C. Foias, Navier-Stokes Equations, University of Chicago Press, 1988.

[32] V. Girault, P.-A. Raviart, Finite Element Methods for the Navier-Stokes Equations, Vol. 5 of Springer Series in Computational Mathematics, Springer-Verlag, Berlin, 1986, theory and algorithms.

[33] F. Boyer, P. Fabrie, Mathematical Tools for the Study of the Incompressible Navier-Stokes Equations andRelated Models, Vol. 183, Springer Science & Business Media, 2012.

[34] J. G. Heywood, R. Rannacher, Finite-element approximation of the nonstationary navier–stokes problem. part iv: error analysis for second-order time discretization, SIAM Journal on Numerical Analysis 27 (2) (1990) 353–384.

[35] J. Blasco, R. Codina, Error estimates for an operator-splitting method for incompressible flows, Applied Numerical Mathematics 51 (1) (2004) 1–17.

[36] J. Shen, On error estimates of projection methods for navier–stokes equations: first-order schemes, SIAM Journal on Numerical Analysis 29 (1) (1992) 57–77.

[37] T. Zhang, D. Pedro, J. Yuan, A large time stepping viscosity-splitting finite element method for the viscoelastic flow problem, Adv. Comput. Math. 41 (1) (2015) 149–190.

[38] F. Guillén-González, M. V. Redondo-Neble, New error estimates for a viscosity-splitting scheme in time for the three-dimensional Navier-Stokes equations, IMA J. Numer. Anal. 31 (2) (2011) 556–579.

[39] F. Hecht, New development in freefem++, Journal of numerical mathematics 20 (3-4) (2012) 251–266.

[40] A. Masud, J. Kwack, A stabilized mixed finite element method for the incompressible shear-rate dependent non-newtonian fluids: Variational multiscale framework and consistent linearization, Computer methods in applied mechanics and engineering 200 (5-8) (2011) 577–596.

[41] W. Rudin, Principles of mathematical analysis, McGraw Hill, 1953.